NATIONAL ADVISORY COMMITTEE FOR AERONAUTICS

REPORT 947

THE DEVELOPMENT OF CAMBERED AIRFOIL SECTIONS HAVING FAVORABLE LIFT CHARACTERISTICS AT SUPERCRITICAL MACH NUMBERS

By DONALD J. GRAHAM

1949

For sale by the Superintendent of Documents, U. S. Government Printing Office, Washington 25, D. C. Yearly subscription, $3; foreign, $4.50; single copy price varies according to size. - - - - - - - - - Price 20 cents

AERONAUTIC SYMBOLS

1. FUNDAMENTAL AND DERIVED UNITS

	Symbol	Metric		English	
		Unit	Abbreviation	Unit	Abbreviation
Length	l	meter	m	foot (or mile)	ft (or mi)
Time	t	second	s	second (or hour)	sec (or hr)
Force	F	weight of 1 kilogram	kg	weight of 1 pound	lb
Power	P	horsepower (metric)		horsepower	hp
Speed	V	kilometers per hour	kph	miles per hour	mph
		meters per second	mps	feet per second	fps

2. GENERAL SYMBOLS

W Weight $=mg$

g Standard acceleration of gravity $=9.80665$ m/s^2 or 32.1740 ft/sec^2

m Mass $=\frac{W}{g}$

I Moment of inertia $=mk^2$. (Indicate axis of radius of gyration k by proper subscript.)

μ Coefficient of viscosity

ν Kinematic viscosity

ρ Density (mass per unit volume)

Standard density of dry air, 0.12497 kg-m^{-4}-s^2 at 15° C and 760 mm; or 0.002378 lb-ft^{-4} sec^2

Specific weight of "standard" air, 1.2255 kg/m^3 or 0.07651 lb/cu ft

3. AERODYNAMIC SYMBOLS

S Area

S_w Area of wing

G Gap

b Span

c Chord

A Aspect ratio, $\frac{b^2}{S}$

V True air speed

q Dynamic pressure, $\frac{1}{2}\rho V^2$

L Lift, absolute coefficient $C_L=\frac{L}{qS}$

D Drag, absolute coefficient $C_D=\frac{D}{qS}$

D_0 Profile drag, absolute coefficient $C_{D_0}=\frac{D_0}{qS}$

D_i Induced drag, absolute coefficient $C_{D_i}=\frac{D_i}{qS}$

D_p Parasite drag, absolute coefficient $C_{D_p}=\frac{D_p}{qS}$

C Cross-wind force, absolute coefficient $C_C=\frac{C}{qS}$

i_w Angle of setting of wings (relative to thrust line)

i_t Angle of stabilizer setting (relative to thrust line)

Q Resultant moment

Ω Resultant angular velocity

R Reynolds number, $\rho\frac{Vl}{\mu}$ where l is a linear dimension (e.g., for an airfoil of 1.0 ft chord, 100 mph, standard pressure at 15° C, the corresponding Reynolds number is 935,400; or for an airfoil of 1.0 m chord, 100 mps, the corresponding Reynolds number is 6,865,000)

α Angle of attack

ϵ Angle of downwash

α_0 Angle of attack, infinite aspect ratio

α_i Angle of attack, induced

α_a Angle of attack, absolute (measured from zero-lift position)

γ Flight-path angle

REPORT 947

THE DEVELOPMENT OF CAMBERED AIRFOIL SECTIONS HAVING FAVORABLE LIFT CHARACTERISTICS AT SUPERCRITICAL MACH NUMBERS

By DONALD J. GRAHAM

Ames Aeronautical Laboratory
Moffett Field, Calif.

National Advisory Committee for Aeronautics

Headquarters, 1724 F Street NW., Washington 25, D. C.

Created by act of Congress approved March 3, 1915, for the supervision and direction of the scientific study of the problems of flight (U. S. Code, title 50, sec. 151). Its membership was increased from 12 to 15 by act approved March 2, 1929, and to 17 by act approved May 25, 1948. The members are appointed by the President, and serve as such without compensation.

TECHNICAL COMMITTEES

AERODYNAMICS
POWER PLANTS FOR AIRCRAFT
AIRCRAFT CONSTRUCTION
OPERATING PROBLEMS
INDUSTRY CONSULTING

Coordination of Research Needs of Military and Civil Aviation
Preparation of Research Programs
Allocation of Problems
Prevention of Duplication
Consideration of Inventions

LANGLEY AERONAUTICAL LABORATORY
Langley Field, Va.

LEWIS FLIGHT PROPULSION LABORATORY
Cleveland Airport, Cleveland, Ohio

AMES AERONAUTICAL LABORATORY
Moffett Field, Calif.

Conduct, under unified control, for all agencies of scientific research on the fundamental problems of flight

OFFICE OF AERONAUTICAL INTELLIGENCE
Washington, D. C.

Collection, classification, compilation, and dissemination of scientific and technical information on aeronautics

REPORT 947

THE DEVELOPMENT OF CAMBERED AIRFOIL SECTIONS HAVING FAVORABLE LIFT CHARACTERISTICS AT SUPERCRITICAL MACH NUMBERS

By Donald J. Graham

SUMMARY

Several groups of new airfoil sections, designated as the NACA 8-series, are derived analytically to have lift characteristics at supercritical Mach numbers which are favorable in the sense that the abrupt loss of lift, characteristic of the usual airfoil section at Mach numbers above the critical, is avoided. Aerodynamic characteristics determined from two-dimensional wind-tunnel tests at Mach numbers up to approximately 0.9 are presented for each of the derived airfoils. Comparisons are made between the characteristics of these airfoils and the corresponding characteristics of representative NACA 6-series airfoils.

The experimental results confirm the design expectations in demonstrating for the NACA 8-series airfoils either no variation, or an increase from the low-speed design value, in the lift coefficient at a constant angle of attack with increasing Mach number above the critical. It was not found possible to improve the variation with Mach number of the slope of the lift curve for these airfoils above that for the NACA 6-series airfoils. The drag characteristics of the new airfoils are somewhat inferior to those of the NACA 6-series with respect to divergence with Mach number, but the pitching-moment characteristics are more favorable for the thinner new sections in demonstrating somewhat smaller variations of moment coefficient with both angle of attack and Mach number.

The effect on the aerodynamic characteristics at high Mach numbers of removing the cusp from the trailing-edge regions of two 10-percent-chord-thick NACA 8-series airfoils is determined to be negligible.

The use of a negatively deflected plain flap at supercritical Mach numbers on an NACA 6-series airfoil is indicated to be a feasible and promising means for obtaining on demand the favorable variation with Mach number of the lift coefficient at a given angle of attack, characteristic of the NACA 8-series airfoils, while retaining at all other times the superior drag characteristics of the NACA 6-series type of airfoil.

INTRODUCTION

The usual positively cambered airfoil sections exhibit two particularly undesirable characteristics at supercritical Mach numbers. The angle of attack corresponding to the design lift coefficient increases rapidly with increasing Mach number above that for lift divergence, and the lift-curve slope decreases sharply at these Mach numbers. The effects of these characteristics on airplanes employing such wing sections is to alter, respectively, the longitudinal trim and the longitudinal stability and controllability in such a manner as to promote serious airplane diving attitudes, recovery from which may be extremely difficult with normal controls. (See reference 1.) On light highly maneuverable aircraft, these characteristics can be avoided or satisfactorily coped with by the use of symmetrical airfoil sections and special controls. Neither of these means is advisable for large heavily loaded aircraft, however; the first, because in this case the airfoil must of necessity carry some design lift, and the second, because, as is stated in reference 1, the trim changes occur so abruptly that the aircraft would be subjected to dangerously high accelerations before the controls could be reset. The logical means for avoiding the trim and stability changes on large airplanes is the employment of airfoil sections having no adverse changes with Mach number of the angle of attack for the design lift coefficient and of the slope of the lift curve. The development of airfoils having such characteristics at supercritical Mach numbers has accordingly been made the subject of an intensive search.

Although it has not yet been found possible to control the variation with Mach number of the lift-curve slope, a means for achieving a favorable variation with Mach number of the lift of a positively cambered airfoil at the design attitude has been conceived by H. Julian Allen of the Ames Aeronautical Laboratory. This principle has been employed to derive analytically a new group of airfoil sections, designated the NACA 8–series. The aerodynamic characteristics of these airfoils have been determined experimentally in the Ames 1- by 3½-foot high-speed wind tunnel, and the results have, in most cases, confirmed the design expectations. An account of the airfoil development, analytical and experimental, is the subject of the present report.

AIRFOIL DEVELOPMENT

It was observed early in the course of investigations of compressibility effects on airfoil characteristics that the initial loss in lift (sometimes termed the "shock stall") experienced at supercritical Mach numbers was associated with the formation of a compression shock wave on the upper surface of an airfoil before the critical Mach number of the lower surface had been exceeded. It has been concluded that the loss in lift results from an effective change in the airfoil camber occasioned by a suddenly thickened boundary layer behind the

shock wave on the upper surface while the boundary layer on the lower surface remains sensibly unchanged. Previous research has been aimed at continuously increasing the Mach number of occurrence of the compression shock so as to delay the shock stall. In the present development the upper-surface shock wave is accepted, but the associated loss in airfoil lift is forestalled by inducing a corresponding shock, with accompanying boundary-layer growth, to occur on the lower surface.

It was reasoned that if the flow over both surfaces could be kept similar at supercritical Mach numbers the net lift of an airfoil could be maintained at an approximately constant design value. To effect this result the respective minimum pressures on the upper and lower surfaces would have to be equal. Because the drag characteristics at supercritical Mach numbers would be adversely affected by simultanous occurrence of compression shocks on the respective surfaces, it would be desirable to obtain the highest possible airfoil critical Mach number. It was further realized that, to produce a positive lift force on the airfoil at supercritical Mach numbers under this condition, the position of minimum pressure would have to be located farther aft on the lower surface than on the upper surface. The respective upper- and lower- surface minimum pressures being equal, a more severe adverse pressure gradient would thus be imposed aft of the minimum pressure position on the lower surface, forcing a greater thickening of the boundary layer on this surface at Mach numbers above the critical. The effect of the thickened lower-surface boundary layer should compensate, to a degree depending upon the respective upper- and lower-surface velocity distributions, for the upper-surface boundary-layer growth and result in either no change or an effectively positive change in the airfoil camber at Mach numbers above the critical. It was therefore concluded that, by suitably choosing the velocity distributions over the upper and lower surfaces, airfoil sections could be designed to have, at a given angle of attack, an approximately constant or an increased lift at supercritical Mach numbers.

Following this line of reasoning, an initial group of three NACA 8-series airfoil sections, 16-percent-chord-thick, having different respective positions of minimum pressure (or maximum local velocity) on the upper and lower surfaces was designed and tested. The sections were derived in essentially the same manner as were the later families of NACA airfoils by combining mean camber lines with basic thickness forms to produce a desired velocity distribution. Velocity distributions were selected to provide the desired aerodynamic characteristics at supercritical Mach numbers, and the airfoil shapes corresponding to these distributions were determined by the method of reference 2.

The first airfoil was proportioned to have equal upper- and lower-surface minimum pressures occurring at 30 and 50 percent of the chord, respectively. The base profile was obtained by combining proper fractions of the thickness forms of the NACA 63- and 65-series airfoils and the "double-roof" profiles of reference 2. A mean camber line satisfying the condition of equal minimum pressures for the upper and lower surfaces was determined by combining suitable proportions of the NACA $a=0.3$, 0.5, and 1.0 mean lines. (See reference 3.) The ordinates of the mean camber line were adjusted to produce the desired design lift coefficient. The actual airfoil shape was then obtained by combining the base profile with the mean camber line, using the methods of references 2 and 3.

In the manner described three airfoil sections were derived with different respective upper- and lower-surface minimum-pressure positions so located as to permit the effects of a variation of the severity of the lower-surface pressure recovery to be observed. The airfoils were designated as follows:

NACA 835A216
NACA 836A216
NACA 847A216

The shapes and velocity distributions for these airfoils are illustrated in figure 1.

The numbering system for these airfoils is identical with that given in reference 3 for the NACA 7-series airfoils and is summarized as follows:

1st digit— Airfoil series number
2nd digit—Position of minimum pressure on upper surface in tenths of chord from leading edge
3rd digit— Position of minimum pressure on lower surface in tenths of chord from leading edge
Letter— Serial letter distinguishing airfoils having the same thickness, design lift coefficient and minimum pressure positions but different camber or thickness distributions
4th digit —Design lift coefficient in tenths
5th ond 6th digits—Thickness-chord ratio in hundredths

Tests of the initial three airfoils revealed variations in lift coefficient with Mach number in the vicinity of the design lift coefficient which at supercritical Mach numbers differed in important aspects from the type of variation normally observed for airfoil sections. The lift coefficient at a constant angle of attack increased markedly with increasing Mach number above that for normal lift divergence as contrasted with the usually noted opposite variation. Instead of decreasing with increasing Mach number above that for normal lift divergence, the lift coefficient at a constant angle of attack increased markedly with Mach number. This result confirmed the design expectations to a greater degree than anticipated, and indicated that great difficulty would be experienced in trimming an airplane using such wing sections at any but positive lift coefficients at supercritical Mach numbers, an important safety feature for large heavily loaded aircraft. This characteristic was unfortunately accompanied by erratic and, from the standpoint of airplane controllability, undesirable variations with Mach number of the slopes of the lift curves.

The desired type of supercritical speed lift characteristic having been realized, efforts were directed toward the derivation of thinner sections with modified camber so as to produce less powerful lift changes at supercritical Mach numbers. A group of 10-percent-chord-thick profiles was accordingly derived from the NACA 836A216 airfoil, this section among those tested having the most favorable characteristics at low

and moderate lift coefficients. This second group of airfoil sections was composed of the following:

NACA 836A110
NACA 836B110
NACA 836C110
NACA 836D110

The NACA 836A110 airfoil was scaled down in thickness from the NACA 836A216 airfoil and the camber-line ordinates were adjusted to give a design lift coefficient of 0.1. Tests of this airfoil disclosed the need for modification of both the thickness and the camber distribution, the gain in lift at supercritical Mach numbers still being greater than desirable.

It was reasoned that, by decreasing the negative lift carried over the rear portion of the airfoil at subcritical Mach numbers, the change in the total lift of the airfoil at supercritical Mach numbers would be reduced. The NACA 836B110 airfoil was designed to effect this result by modifying both the mean camber line and the thickness distribution of the NACA 836A110 arifoil. The mean camber line for the former was obtained as the sum of equal proportions of the ordinates and slopes of the mean line for the latter airfoil, and of a uniform load ($a=1.0$) mean line. The upper- and lower-surface minimum pressures were maintained approximately equal by adding to one-half of the base profile ordinates of the NACA 836A110 airfoil, one-half of those for the NACA 66–010 airfoil. The resulting changes in profile and velocity distribution may be noted from an examination of parts (d) and (e) of figure 1.

The NACA 836C110 airfoil was designed to investigate the effect on the supercritical speed aerodynamic characteristics of the NACA 836B110 airfoil of removing the cusp from the rear portion of the profile. The former differs from the NACA 836B110 airfoil only in that the profile is linear over approximately the last two-tenths of the chord.

Tests of the NACA 836B110 airfoil indicated that the profile modification from the NACA 836A110 airfoil was effective in reducing the magnitude of the lift-coefficient increase at supercritical Mach numbers in the vicinity of the design lift coefficient. Further improvement was still felt to be desirable, however, particularly in the slope of the lift curve at lift coefficients greater than the design value. A decrease in the severity of the pressure recovery over the lower surface (by decreasing the negative pressure peak) was indicated as a possible corrective measure. To test this hypothesis, the NACA 836D110 airfoil was derived by combining the thickness form obtained as the sum of equal proportions of the NACA 836A010 and 63–010 profiles with the mean camber line of the NACA 836B110 airfoil. The difference between the NACA 836B110 and 836D110 airfoils may be seen from figure 1 to be principally in the magnitude of the lower-surface minimum pressure.

To investigate the possibility of realizing improved characteristics from more rearward minimum-pressure positions on both surfaces, three additional 10-percent-chord-thick sections were derived from the NACA 847A216 airfoil and were designated as follows:

NACA 847A110
NACA 847B110
NACA 847C110

The NACA 847A110 airfoil was derived from the NACA 847A216 airfoil by reducing the base-profile ordinates of the latter in the ratio of fifteen-sixteenths times the quotient resulting from the division of the ordinates of the NACA 66–010 airfoil by the ordinates for the NACA 66_2–015 airfoil, and by reducing the camber-line ordinates and slopes in the ratio 10:16. The NACA 847B110 airfoil was obtained by combining the sum of one-half of the base-profile ordinates of the NACA 847A110 airfoil and one-half of those for the NACA 64–010 airfoil with the mean camber line consisting of equal proportions of the slopes and ordinates of the mean line for the NACA 847A110 airfoil and of the uniform load mean line. The NACA 847C110 airfoil consists of the NACA 847B110 airfoil with the cusp removed from the trailing-edge region of the latter by substituting straight lines for the portion of the profile from approximately the 80-percent-chord position to the trailing edge.

The ordinates of all of the airfoils investigated are given in tables I to X. The shapes and theoretical velocity distributions for all but the NACA 836C110 and 847C110 airfoils (which differ but slightly from the NACA 836B110 and 847B110 airfoils, respectively) are illustrated in figure 1.

It is to be noted that negative deflections of a plain trailing-edge flap on an ordinary airfoil section would produce lower-surface velocity distributions approaching in character the distribution previously described for the new type of airfoil section with the reflexed mean camber line. The results of an investigation (also conducted in the Ames 1- by 3½-foot high-speed wind tunnel) of an NACA 65–210 airfoil with a 20-percent-chord negatively deflected flap accordingly are presented and compared in the present report with those for the NACA 8-series profiles.

SYMBOLS

a	mean-line designation, fraction of chord from leading edge over which design load is uniform
a_0	airfoil section lift-curve slope, per degree
c	chord, feet
c_d	section drag coefficient
c_l	section lift coefficient
c_{l_i}	design section lift coefficient
$c_{m_{c/4}}$	section moment coefficient about quarter-chord point
M	Mach number
V	free-stream velocity, feet per second
v	local velocity, feet per second
x	distance along chord, feet
y	distance perpendicular to chord, feet
α_0	section angle of attack, degrees
α_i	section angle of attack corresponding to design lift coefficient, degrees
δ_f	flap deflection, degrees

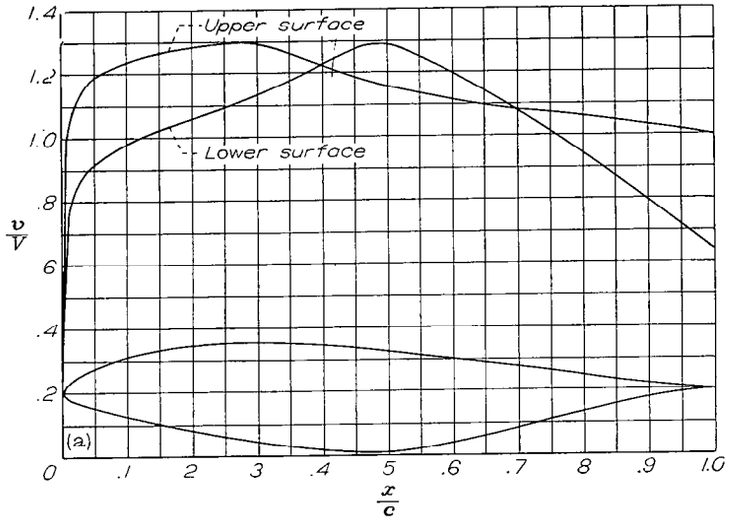

(a) NACA 835A216 airfoil.

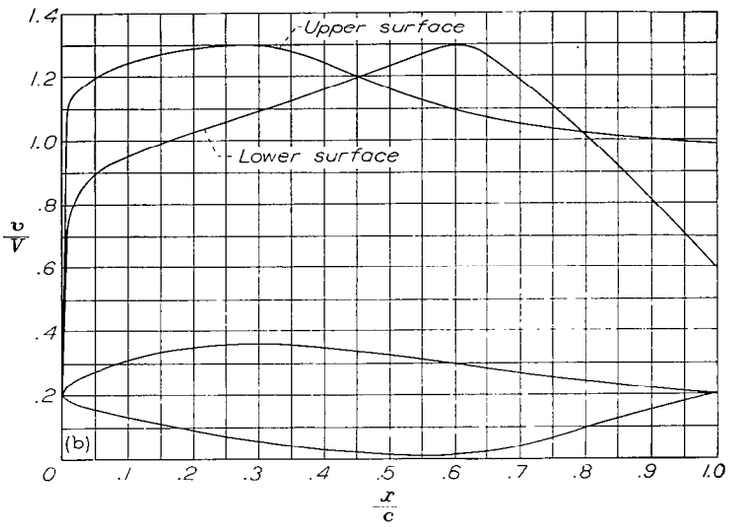

(b) NACA 836A216 airfoil.

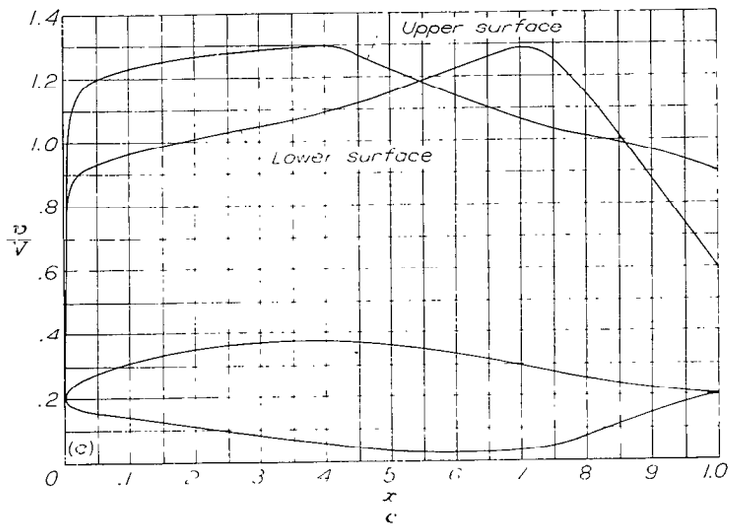

(c) NACA 847A216 airfoil.

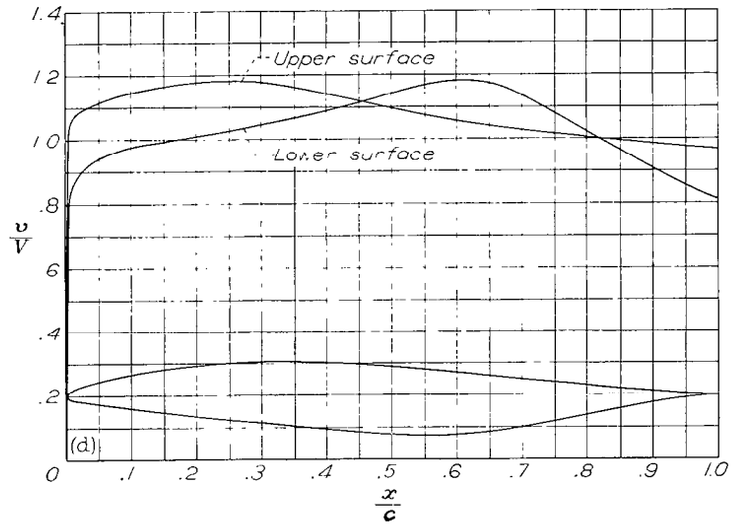

(d) NACA 836A110 airfoil.

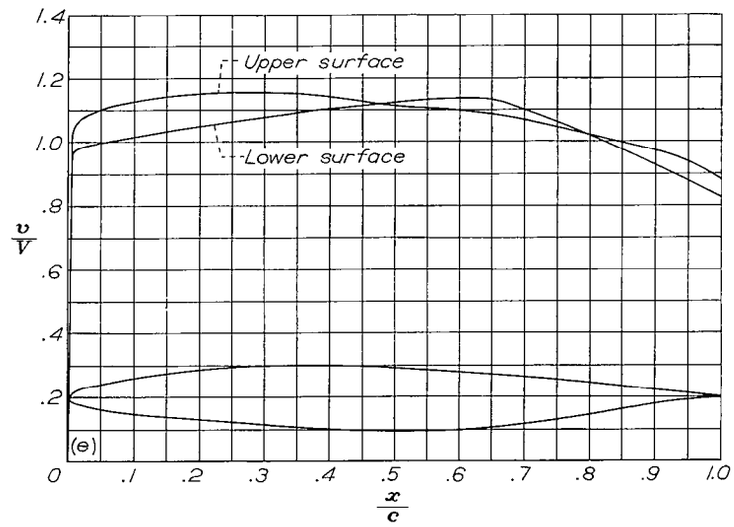

(e) NACA 836B110 airfoil.

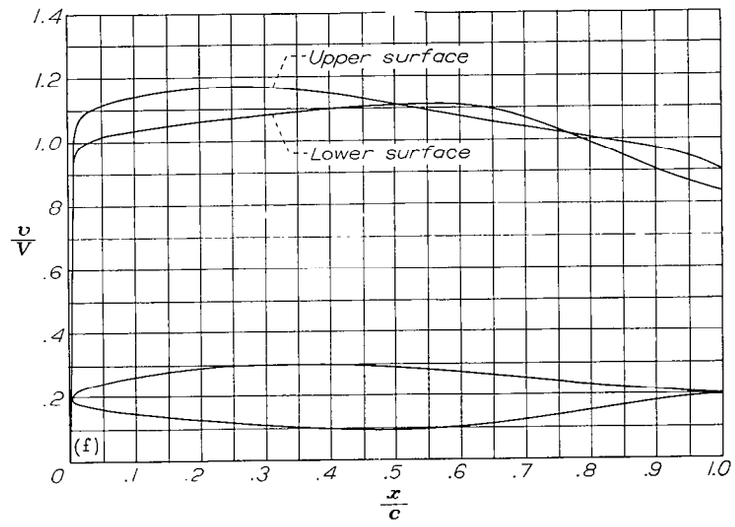

(f) NACA 836D110 airfoil.

FIGURE 1.—Theoretical velocity distributions and profiles for the NACA 8-series airfoils.

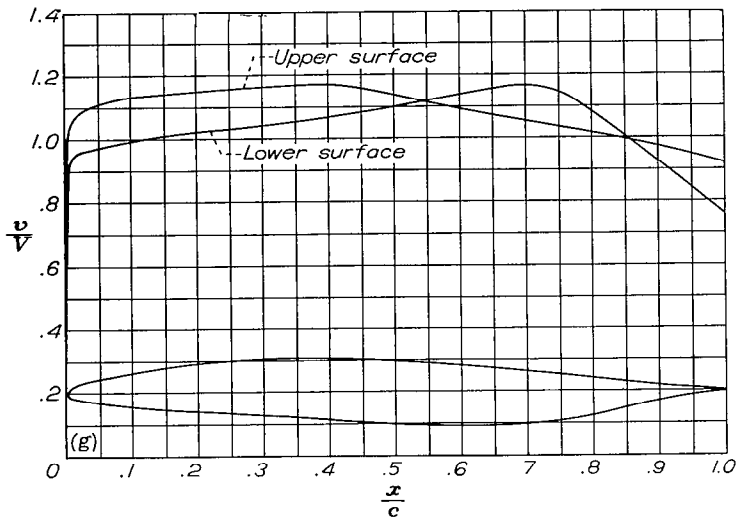

(g) NACA 847A110 airfoil.

FIGURE 1.—Continued.

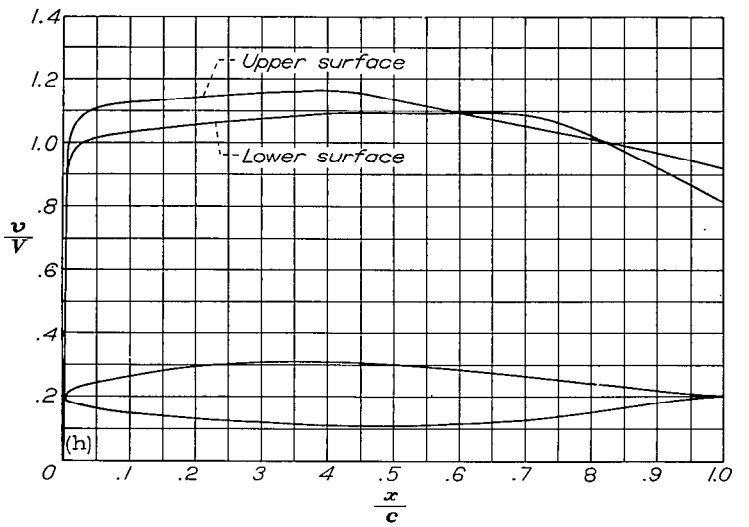

(h) NACA 847B110 airfoil.

FIGURE 1.—Concluded.

APPARATUS AND TESTS

The tests were made in the Ames 1- by 3½-foot high-speed wind tunnel, a low-turbulence, two-dimensional-flow wind tunnel.

The airfoil models were accurately constructed of aluminum alloy and were of 6-inch chord and 12-inch span. The models completely spanned the narrow dimension of the tunnel test section. Two-dimensional flow was assured through the use of sponge-rubber gaskets (to prevent end leakage) compressed between the model ends and the tunnel walls.

Measurements of lift, drag, and quarter-chord pitching moment were made as nearly simultaneously as possible at Mach numbers ranging from 0.3 to as high as 0.9 for each of the airfoils at angles of attack increasing by 2° increments from −6° to a maximum of 12°. The Reynolds number variation with Mach number for the tests is expressed graphically in figure 2.

Lift and pitching moments were evaluated by a method similar to that described in reference 3 from integrations of the pressure reactions on the floor and ceiling of the tunnel of the forces on the airfoils. Drag values were determined from wake-survey measurements made with a rake of total-head tubes.

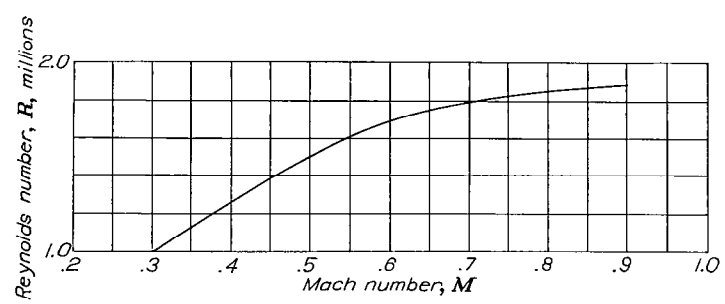

FIGURE 2.—The variation of Reynolds number with Mach number for tests of 6-inch-chord airfoil models in the Ames 1- by 3½-foot high-speed wind tunnel.

RESULTS AND DISCUSSION

Section aerodynamic characteristics in coefficient form are presented as functions of Mach number in figures 3 to 47 for the NACA 8-series airfoils, two representative NACA 6-series airfoils, and the NACA 65–210 airfoil with a 20-percent-chord plain trailing-edge flap neutral and negatively deflected through 6°. All the characteristics are shown corrected for tunnel-wall interference by the methods of reference 4. The dashed portions of the airfoil characteristics curves serve to indicate the extent of possibly unreliable data obtained in the close vicinity of Mach numbers for which the flow in the tunnel test section was choked, that is, for which the Mach number of unity was attained locally across the test section.

CHARACTERISTICS OF INITIAL THREE AIRFOILS

It is seen from figures 3, 4, and 5 that the respective variations with Mach number of the lift coefficient at constant angles of attack for the NACA 835A216, 836A216, and 847A216 airfoils differ markedly from the variations generally observed for ordinary airfoil sections. An abrupt increase of large magnitude occurs in the lift coefficient at angles of attack within the normally useful range at Mach numbers above those for lift divergence in place of the customary decrease in lift coefficient. The difference in characteristics is emphasized in figure 6 which illustrates the variation with Mach number of the angle of attack required to maintain the design lift coefficient of 0.2 for each of these NACA 8-series airfoils, and for the NACA 65_2–215, $a=0.5$ airfoil (see reference 5), a representative NACA 6-series airfoil.

The explanation for the radical lift characteristics of the new airfoils is to be found in an examination of the theoretical low-speed velocity distributions of figure 1. At Mach numbers above the critical the strong adverse pressure gradient aft of the minimum-pressure position on the lower surface promotes a rapid thickening and separation of the

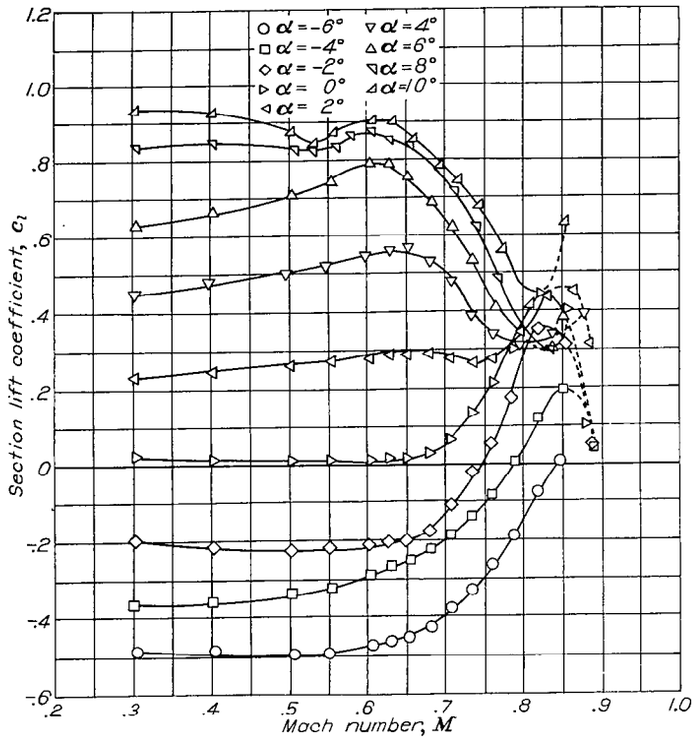

FIGURE 3.—The variation of section lift coefficient with Mach number at various angles of attack for the NACA 835A216 airfoil.

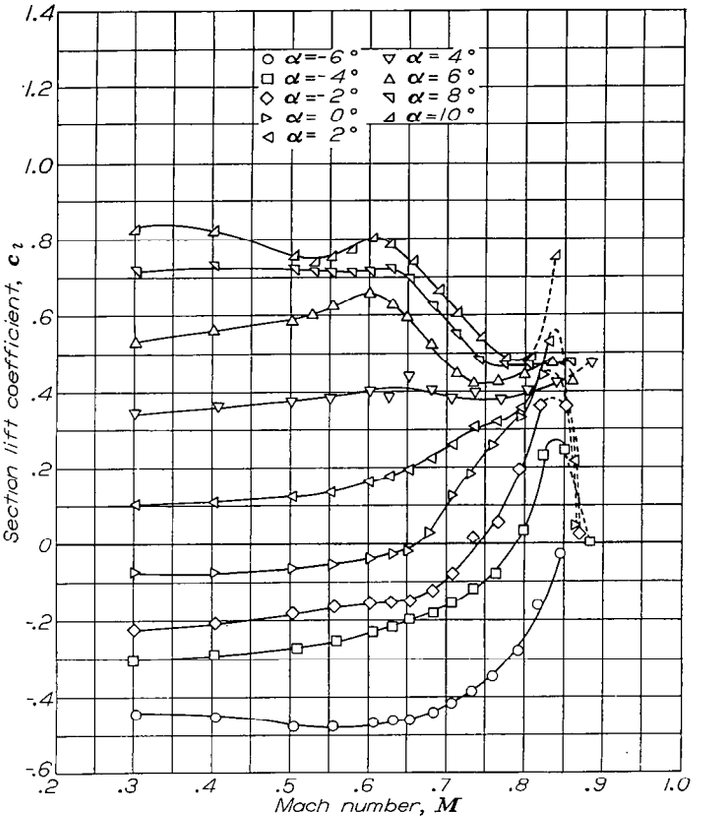

FIGURE 4.—The variation of section lift coefficient with Mach number at various angles of attack for the NACA 836A216 airfoil.

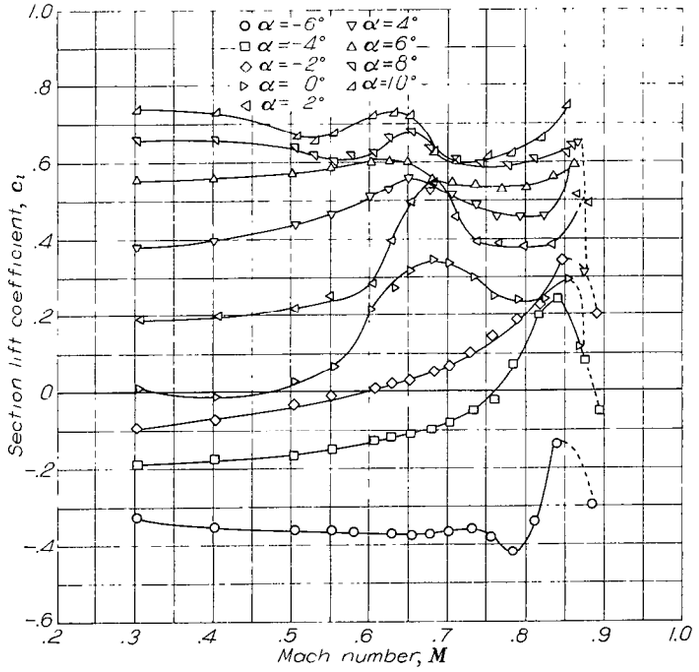

FIGURE 5.—The variation of section lift coefficient with Mach number at various angles of attack for the NACA 847A216 airfoil.

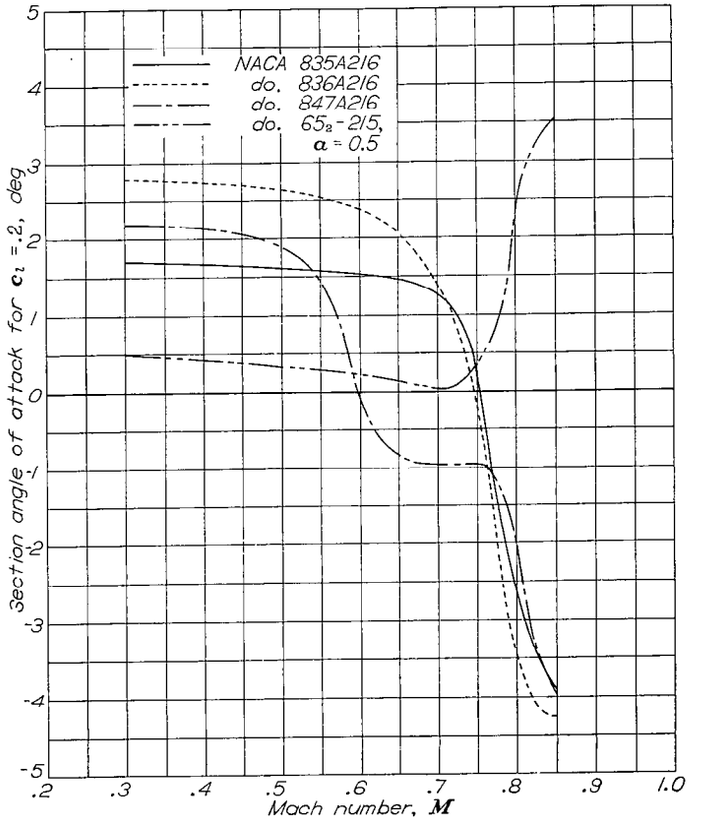

FIGURE 6.—The variation with Mach number of the section angle of attack for a lift coefficient of 0.2 for the NACA 835A216, 836A216, 847A216 and 65_2-215. a=0.5, airfoils.

boundary layer from this surface, resulting in the loss of an extensive portion of the negative lift carried over that part of the airfoil immediately aft of the lower-surface minimum-pressure position. The increasing extent of the separation on the lower surface with increasing Mach number produces the increasingly positive variation of lift coefficient at constant angles of attack observed in figures 3, 4, and 5.

The variation with Mach number of the lift coefficient at low positive and negative angles of attack, although favorable in the sense that the lift coefficient increases with Mach number rather than decreases, is so violent for these three airfoils as to cause very erratic and undesirable variations in the slope of the lift curve at the higher Mach numbers. (See fig. 7.) The variation of the angle of attack necessary to maintain the design lift coefficient of 0.2, although in the direction to promote safety at high Mach numbers for an airplane employing such airfoils as wing sections, has already been observed in figure 6 to be undesirably large. For these reasons it was concluded that the first airfoils were cambered too severely and that a modified amount of camber as well as a change in the distribution would produce less drastic changes in the lift coefficient with increasing Mach number.

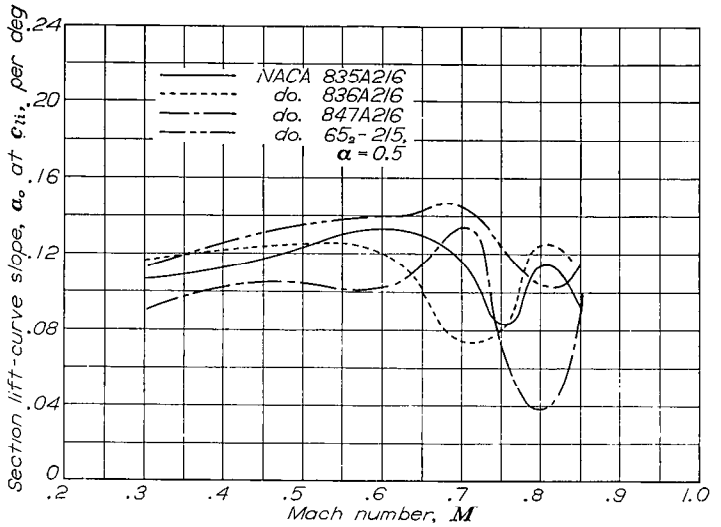

FIGURE 7.—The variation with Mach number of the section lift-curve slope at the design lift coefficient for the NACA 835A216, 836A216, 847A216 and 65_2–215, $a=0.5$, airfoils.

The drag characteristics of the three airfoils (figs. 8, 9, and 10), as was expected, are much inferior to those of the NACA 6-series airfoils, as represented in reference 5 by the NACA 65_2–215, $a=0.5$ and NACA 66,2–215, $a=0.6$ airfoils, with respect to divergence with increasing Mach number at low and moderate angles of attack despite allowance for the small difference in thickness of the airfoils.

The variation of pitching-moment coefficient with Mach number for the NACA 835A216, 836A216, and 847A216 airfoils, shown in figures 11, 12, and 13, respectively, is consistent with the variation of lift coefficient. The moment coefficients vary from positive values at low Mach numbers where negative lift is carried over the rearward portion of the airfoil to negative values at high Mach numbers where this negative lift is lost.

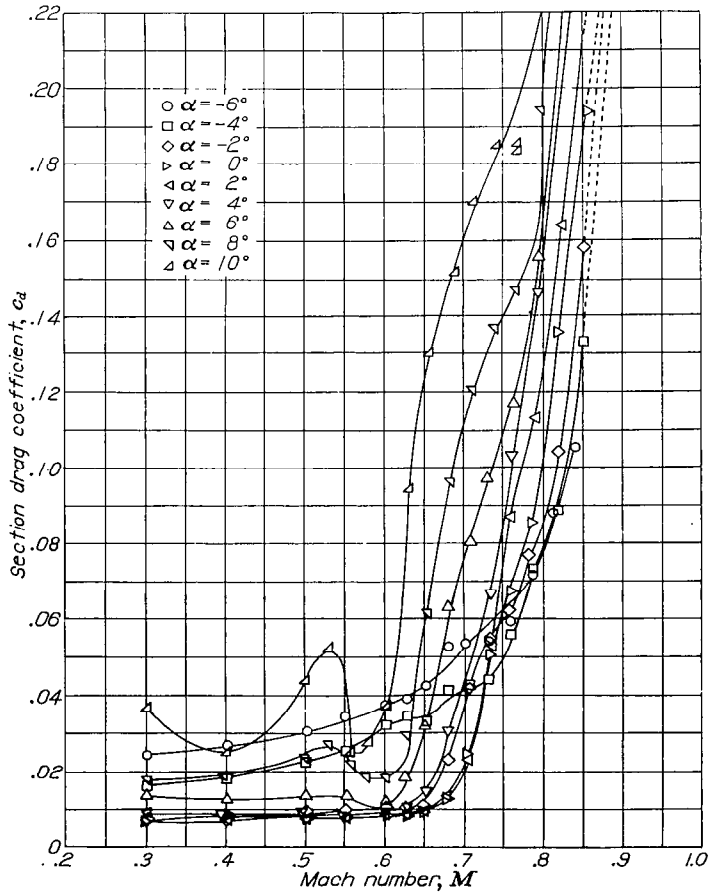

FIGURE 8.—The variation of section drag coefficient with Mach number at various angles of attack for the NACA 835A216 airfoil.

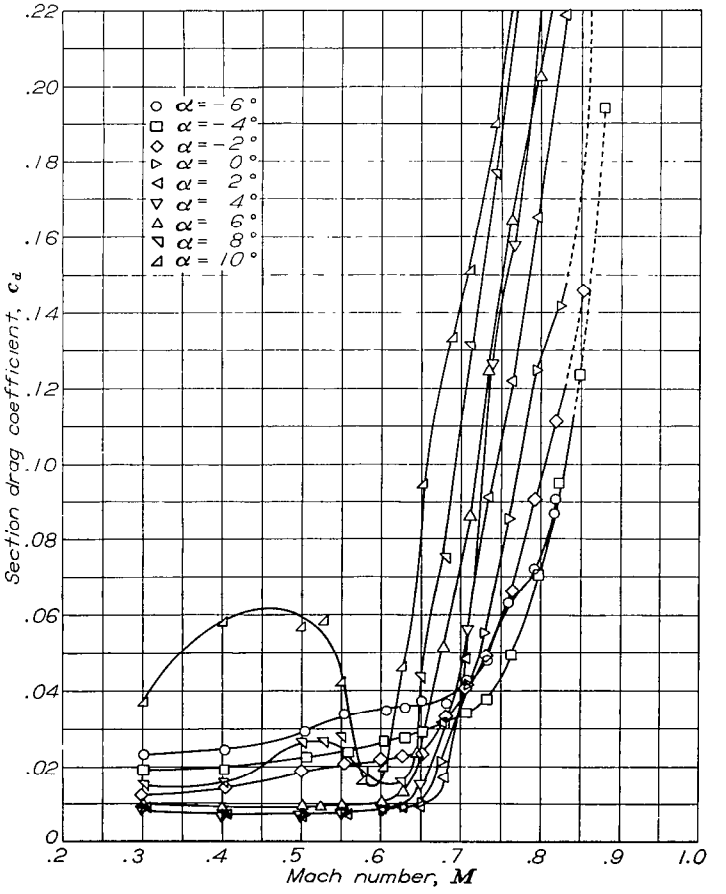

FIGURE 9.—The variation of section drag coefficient with Mach number at various angles of attack for the NACA 836A216 airfoil.

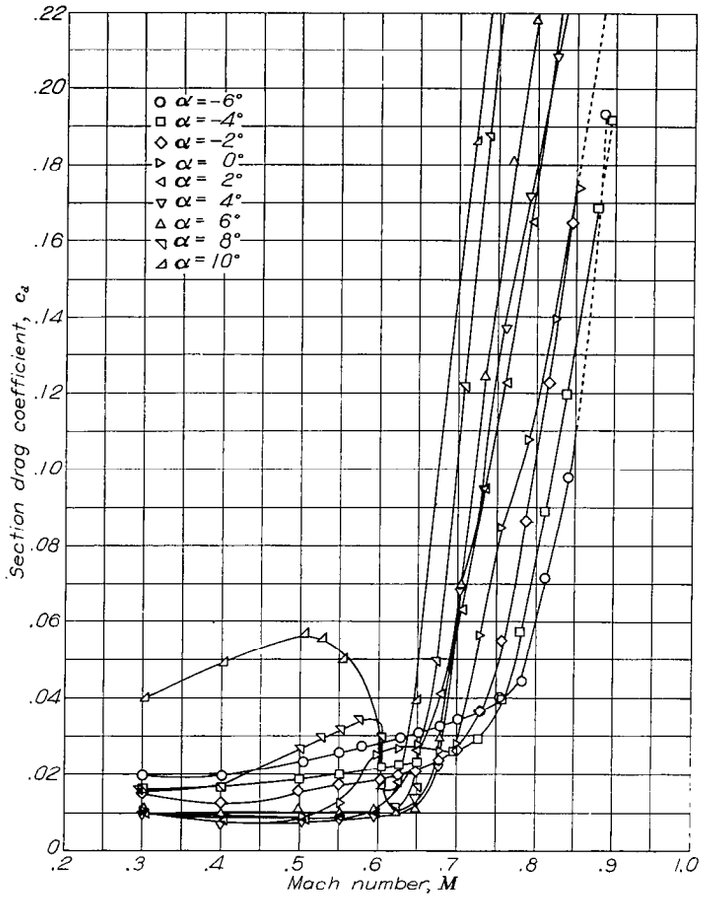

FIGURE 10.—The variation of section drag coefficient with Mach number at various angles of attack for the NACA 847A216 airfoil.

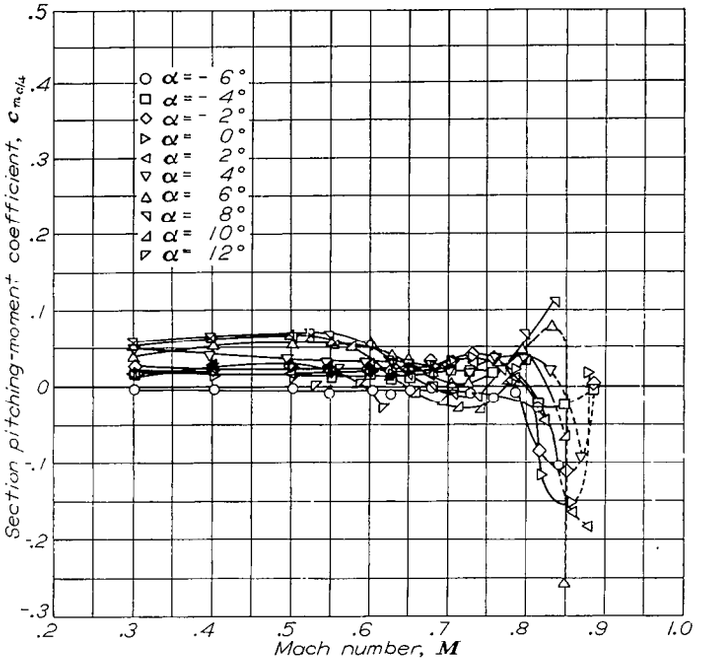

FIGURE 11.—The variation of section quarter-chord moment coefficient with Mach number at various angles of attack for the NACA 835A216 airfoil.

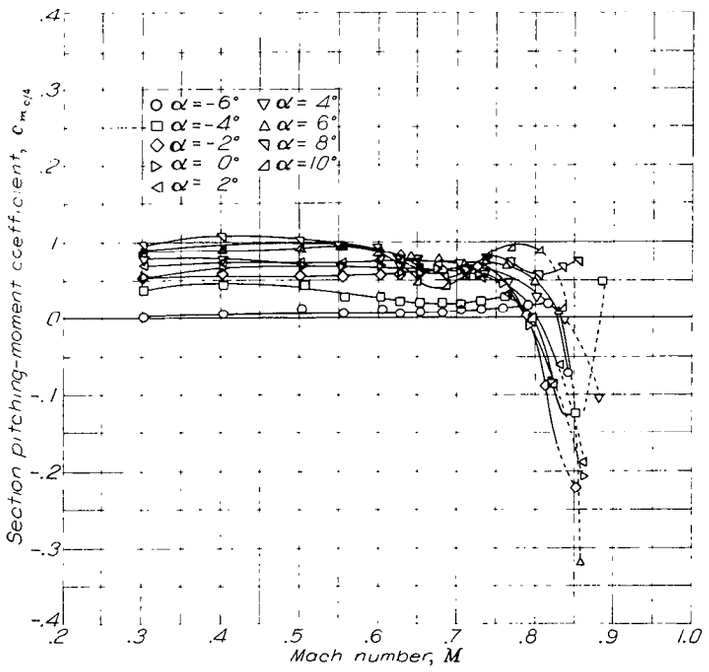

FIGURE 12.—The variation of section quarter-chord moment coefficient with Mach number at various angles of attack for the NACA 836A216 airfoil.

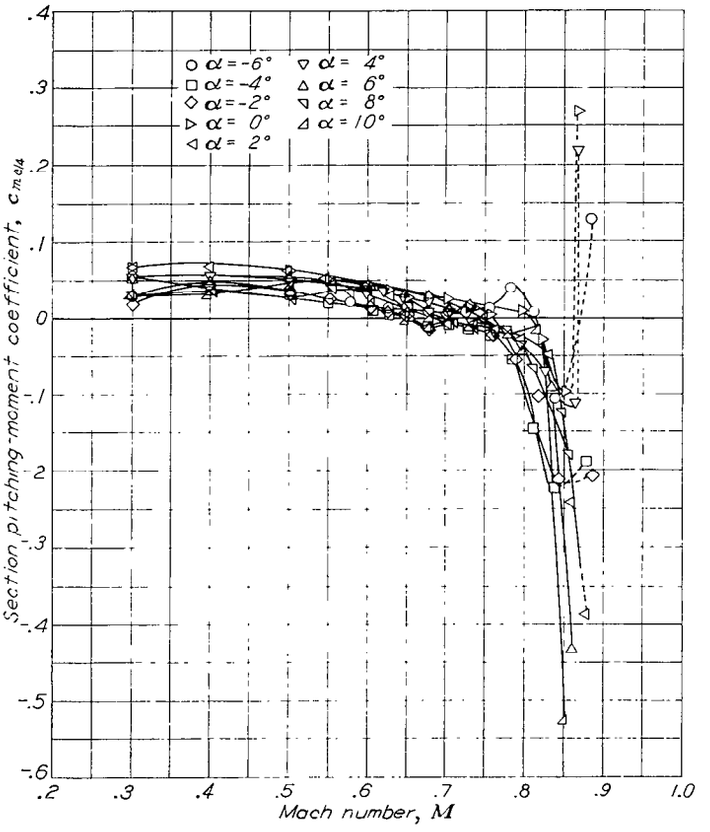

FIGURE 13.—The variation of section quarter-chord moment coefficient with Mach number at various angles of attack for the NACA 847A216 airfoil.

CHARACTERISTICS OF THE NACA 836-110 AIRFOILS

NACA 836A110.—Because current design trends indicate thinner wing sections for high Mach number applications, it was considered desirable to further the investigation on airfoil sections of 10-percent-chord maximum thickness. The effect of halving the amount of camber and decreasing the profile thickness of the NACA 836A216 airfoil may be seen from an examination of the characteristics of the NACA 836A110 airfoil.

The variation of lift coefficient with Mach number for this airfoil (fig. 14) is much less drastic at supercritical Mach numbers than that noted in figure 3 for the NACA 836A216 airfoil. The lift-curve-slope variation with Mach number is considerably improved for the NACA 836A110 airfoil (cf., figs. 7 and 19), and the angle of attack required to maintain the lift coefficient at the design value (cf., figs. 6 and 20) is correspondingly reduced for the thinner lower-cambered profile. The latter variation is still undesirably large, however.

The differences in the lift characteristics of the NACA 836A110 airfoil and the NACA 64–110 airfoil, as representative of the best NACA 6-series sections for high Mach number applications, may be seen from a comparison of figures 14 and 18 to lie in the variations of lift coefficient with Mach number at small positive and negative angles of attack. The departure of the characteristics of the former airfoil from those usually observed for airfoil sections at supercritical Mach numbers is more strikingly illustrated in figure 20, depicting the variation with Mach number of the angle of attack required to maintain the design lift coefficient of 0.1 for the NACA 836–110 and 64–110 airfoil sections.

The drag and pitching-moment characteristics of the NACA 64–110 airfoil section at high Mach numbers being unavailable at the present writing, these characteristics for the NACA 836A110 airfoil must be compared with those for the NACA 65-210 airfoil as the next most representative profile of the NACA 6-series airfoils available. The drag characteristics of the NACA 836A110 airfoil (fig. 21) compare unfavorably with those of the NACA 65–210 airfoil (fig. 25), particularly at the angles of attack corresponding to the lower lift coefficients. Divergence not only occurs earlier for the former, but the drag coefficients at a given lift coefficient are higher.

From figures 26 and 30, respectively, the pitching-moment coefficients for the NACA 836A110 airfoil, in addition to being more positive, exhibit a generally smaller variation with Mach number than do those for the NACA 65-210 airfoil.

NACA 836B110.—The NACA 836B110 airfoil was derived from the NACA 836A110 airfoil in such a manner as to reduce the negative lift on the after portion of the airfoil at subcritical Mach numbers at the design lift attitude and to retain the approximately equal critical Mach numbers of the upper and lower surfaces. The effect of these profile modifications on the lift-coefficient variation with Mach number is shown by a comparison of figures 14 and 15. The variation in the vicinity of the design lift coefficient is seen to be small for the NACA 836B110 airfoil as compared with that for the NACA 836A110 airfoil. At angles of attack appreciably above and below the ideal angle, the lift-coefficient variation resembles that observed for the NACA 6-series type of section. (See figs. 18 and 42 for the NACA 64-110 and 65–210 airfoils.)

A considerable increase in the slope of the lift curve at the design lift coefficient is observed in figure 19 for the NACA 836B110 airfoil over that of the NACA 836A110 airfoil for Mach numbers between 0.75 and 0.85. The variation with Mach number of this parameter for the former airfoil is closely comparable to that for the NACA 64–110 airfoil. From figure 20, it can be seen that the variation with Mach number of the angle of attack necessary to maintain the design lift coefficient for the NACA 836B110 airfoil is greatly reduced from that observed for the NACA 836A110 airfoil.

The drag characteristics of the NACA 836B110 airfoil (fig. 22), although considerably improved over those of the NACA 836A110 section, are still inferior with respect to divergence with Mach number in the vicinity of the design lift coefficient to those of the NACA 65–210 airfoil when compared on the basis of equal lift coefficients for the two airfoils.

The variation in pitching-moment coefficient with Mach number (fig. 27) for the NACA 836B110 airfoil closely approaches that for the NACA 65–210 airfoil, as a result of the camber modification from that of the NACA 836A110 airfoil.

NACA 836C110.—This airfoil section was tested to determine the effect on the aerodynamic characteristics of the NACA 836B110 airfoil of removing the cusp from the trailing-edge region of the airfoil. Comparison of the respective variations with Mach number of lift, drag, and pitching-moment coefficients (figs. 16, 23, and 28, respectively) for the NACA 836C110 airfoil with the corresponding variations for the NACA 836B110 airfoil reveals no significant differences in the characteristics of the two sections.

NACA 836D110.—The NACA 836D110 airfoil was designed to investigate the effect of both decreasing the amount of negative design lift from that of the NACA 836A110 airfoil and raising the lower-surface critical Mach number above that of the upper surface (note theoretical velocity distribution, fig. 1) in an attempt to obtain a more favorable variation with Mach number of the slope of the lift curve. Figure 17 indicates the NACA 836D110 airfoil to be the most promising of those yet discussed, virtually no variation with Mach number being manifest in the lift coefficient near the design value. This characteristic is reflected in the small variation with Mach number in the angle of attack required to maintain the design lift coefficient of 0.1. (See fig. 20.) With reference again to figure 17, the variation with Mach number of lift coefficient at constant angles of attack other than that corresponding to the design lift coefficient indicated lift-curve slopes closely resembling those of the NACA 6-series airfoils as represented in figure 18.

Except at the higher lift coefficients, no improvement in drag characteristics from those of the NACA 836B110 airfoil resulted from this profile modification.

The variation with Mach number in the pitching-moment coefficients of the NACA 836D110 airfoil (fig. 29) does not differ noteworthily from those for the other airfoils of the series.

CHARACTERISTICS OF THE NACA 847-110 AIRFOILS

NACA 847A110.—The NACA 847A110 airfoil was derived from the NACA 847A216 section by decreasing the thickness and the camber-line ordinates in the same manner as was done in the case of the NACA 836A110 airfoil. The lift-coefficient variation with Mach number (fig. 31) closely resembles that for the latter airfoil. The variation with Mach number of the angle of attack required to maintain the design lift coefficient (fig. 35) is similar to that observed for the NACA 836A110 airfoil (fig. 20).

The variation in drag coefficient with Mach number (fig. 36) is more favorable for the NACA 847A110 airfoil than for the NACA 836A110 airfoil from the standpoint of divergence with Mach number at angles of attack in the vicinity of the ideal angle.

The pitching-moment-coefficient variation with Mach number for the NACA 847A110 airfoil (fig. 39) is similar to that for the NACA 836A110 airfoil, but the moment coefficients are of smaller magnitude.

NACA 847B110.—The lift characteristics of this airfoil, developed from the NACA 847A110 airfoil by decreasing the negative contribution to the design lift distribution and by decreasing the lower-surface pressure peak below that of the upper surface, are seen from figure 32 to be considerably improved over those of the latter airfoil. As in the case of the NACA 836D110 section, the variation with Mach number of the lift coefficient in the vicinity of the design value is indicated to be very small, and yet a reasonably satisfactory lift-curve slope is retained. (See fig. 34.) The variation with Mach number of the angle of attack for maintenance of the design lift coefficient (fig. 35) is as favorable as that observed for the NACA 836D110 airfoil. A marked improvement in the variation of drag coefficient with Mach number at zero lift is noted from a comparison of figures 36 and 37 for the NACA 847A110 and 847B110 airfoils, respectively. For this condition the drag-coefficient variation of the latter airfoil is superior to that of the NACA 836D110 airfoil. The superiority is considerably reduced at the design lift coefficient and disappears at the higher lift coefficients.

The variation in pitching-moment coefficient with Mach number for the NACA 847B110 airfoil (fig. 40) is observed to be very small in the vicinity of the design lift coefficient and parallels the characteristics of the NACA 836D110 airfoil in this respect.

NACA 847C110.—This airfoil was designed to investigate further the effects on the characteristics at high subsonic Mach numbers of removing the cusp from the trailing-edge region of an airfoil. From figures 33, 34, 35, 37, 38, 40, and 41, the characteristics of the resulting airfoil are seen to be essentially the same as those of the cusped NACA 847B110 profile. From this and the similar result observed in the case of the NACA 836–110 airfoils it is concluded that for 10-percent-chord-thick airfoils of this type of section the aerodynamic characteristics are not materially affected by removal of the cusp from the after portion of the profile.

It is to be noted that in the case of both the NACA 836–110 and the NACA 847–110 airfoil developments the sections having the most favorable lift characteristics are those for which the negative portion of the design lift is small and for which the minimum pressure is somewhat lower on the upper surface than on the lower surface of the airfoil. The latter result is in contradiction to the design assumption that the upper- and lower-surface pressure peaks should be equal. Although it was not found possible to improve the lift-curve-slope variation with Mach number for these airfoils over that characteristic of the NACA 6-series airfoils, the NACA 836D110 and 847B110 profiles are indicated to be the equal of the NACA 6–series type in this respect. The drag characteristics of the best NACA 8–series airfoils thus far derived are not as favorable as those of NACA 6–series airfoils in that the drag-divergence Mach numbers are lower for comparable lift coefficients in the vicinity of the design lift coefficients. The pitching-moment characteristics of the more promising airfoils of the NACA 8–series are, if anything, superior to those of the NACA 6-series in that the variations of moment coefficient with Mach number are generally smaller for the former.

CHARACTERISTICS OF AN AIRFOIL WITH A NEGATIVELY DEFLECTED FLAP

From an examination of the lift characteristics of an NACA 65–210 airfoil section with a 20-percent-chord plain trailing-edge flap, a marked similarity was noted between the variation with Mach number of the lift coefficient at various angles of attack for a small negative flap deflection and the characteristics previously observed for the NACA 8-series airfoils. It would be very desirable to be able, by negatively deflecting a plain flap, to effectively reflex the camber of a wing section on an airplane in flight from the uniform load type at subcritical Mach numbers to something approaching that of an NACA 8-series profile at supercritical Mach numbers. To permit an appraisal of the characteristics of an airfoil with a negatively deflected flap at high Mach numbers, the aerodynamic characteristics of the NACA 65–210 section with a 20-percent-chord plain flap undeflected, and negatively deflected 6°, are presented in figures 42, 25, and 30 and in figures 43, 46, and 47, respectively, for comparison with those of the NACA 8-series airfoils investigated.

The similarity between the respective variations with Mach number in the lift coefficient at a constant angle of attack for the NACA 65–210 airfoil with the flap deflected −6° and the NACA 836D110 and 847B110 airfoils is readily apparent from a comparison of figures 43, 17, and 32. The lift characteristics of the three airfoils are further compared in figures 44 and 45 depicting the respective variations

with Mach number in the lift-curve slope and the angle of attack required to maintain the lift coefficient of 0.1. The similarity between the latter characteristics for the airfoil with the negatively deflected flap and the two NACA 8-series airfoils is unmistakable.

The drag characteristics of the flapped airfoil (fig. 46) are similar to those of the NACA 836D110 and 847B110 airfoils. The pitching-moment characteristics of the three airfoils (figs. 47, 29, and 40) also bear a close resemblance to one another.

The principle of reflexing the camber line by negatively deflecting plain training-edge flaps on NACA 6-series airfoils at supercritical Mach numbers to produce favorable variations in lift coefficient with increasing Mach number on the strength of the results contained herein has already found important application (in an expedient sense) on several high-speed airplanes and merits further investigation.

CONCLUDING REMARKS

A new group of airfoil sections, designated the NACA 8-series, has been developed having favorable lift characteristics at supercritical Mach numbers. Through the use of negative camber over a portion of the airfoil chord it has proved possible to hold the lift coefficient of the new type of airfoil approximately constant at some design value with increasing Mach number to at least 0.9 Mach number, the limit of the present investigation. By suitably choosing the camber and thickness distributions for the airfoils, a particular variation with Mach number of the angle of attack required to maintain a given design lift coefficient can be obtained. No means has been found for improving the lift-curve-slope characteristics of the NACA 8-series airfoils beyond those of the NACA 6-series sections. Although some control can be exercised over the drag and pitching-moment characteristics of the former airfoil sections without adversely affecting the lift characteristics, it is generally necessary to accept drag characteristics somewhat poorer with respect to divergence with Mach number than those of the NACA 6-series airfoils presently used for high Mach number applications. The pitching-moment characteristics of the NACA 8-series airfoils are generally more favorable than those of the NACA 6-series airfoils in that the variations of pitching-moment coefficient with Mach number and angle of attack at supercritical Mach numbers are somewhat smaller for the former.

Flat-sided profiles may be used in place of the cusped trailing-edge profiles on 10-percent-chord-thick NACA 8-series airfoils without significantly altering the aerodynamic characteristics of the airfoils at supercritical Mach numbers.

The lift characteristics of the NACA 8-series airfoils at supercritical Mach numbers can be approximated with NACA 6-series airfoils through the use of negatively deflected plain trailing-edge flaps. This application appears to be a promising means for obtaining on demand the favorable variation with Mach number of the lift coefficient at a given angle of attack, characteristic of the NACA 8-series airfoils, and yet retaining at all other times the superior drag characteristics of the NACA 6-series airfoils.

AMES AERONAUTICAL LABORATORY,
NATIONAL ADVISORY COMMITTEE FOR AERONAUTICS,
MOFFETT FIELD, CALIF., *Sept. 22, 1948.*

REFERENCES

1. Hood, Manly J., and Allen, H. Julian: The Problem of Longitudinal Stability and Control at High Speeds. NACA Rep. 767, 1943.
2. Allen, H. Julian: General Theory of Airfoil Sections Having Arbitrary Shape or Pressure Distribution. NACA Rep. 833, 1945.
3. Abbott, Ira H., von Doenhoff, Albert E., and Stivers, Louis S., Jr.: Summary of Airfoil Data. NACA Rep. 824, 1945.
4. Allen, H. Julian, and Vincenti, Walter G.: Wall Interference in a Two-Dimensional-Flow Wind Tunnel With Consideration of the Effect of Compressibility. NACA Rep. 782, 1944.
5. Graham, Donald J., Nitzberg, Gerald E., and Olsen, Robert N.: A Systematic Investigation of Pressure Distributions at High Speeds Over Five Representative NACA Low-Drag and Conventional Airfoil Sections. NACA Rep. 832, 1945.

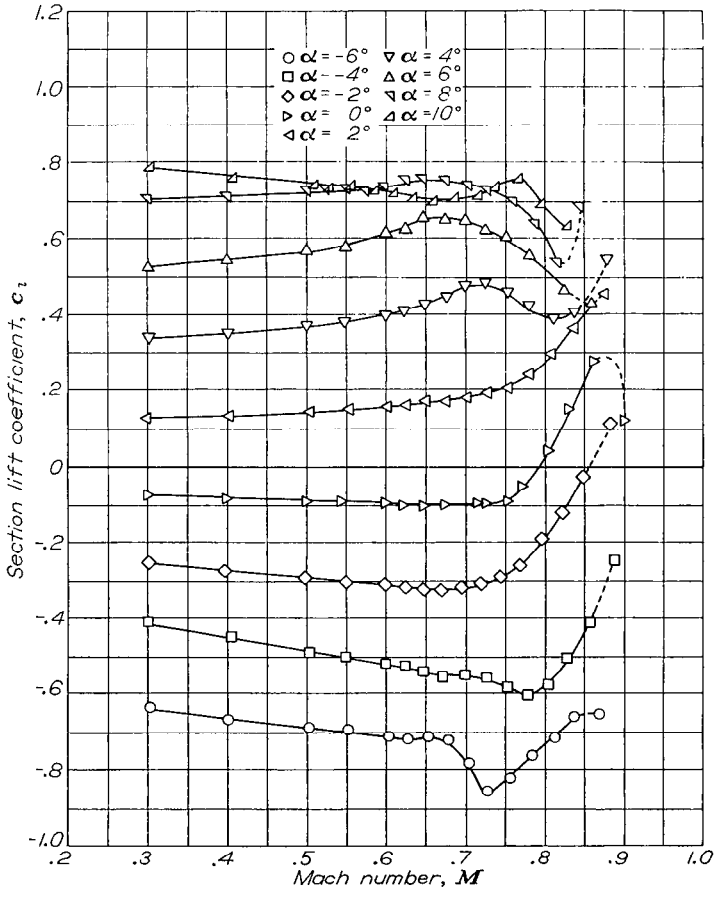

FIGURE 14.—The variation of section lift coefficient with Mach number at various angles of attack for the NACA 836A110 airfoil.

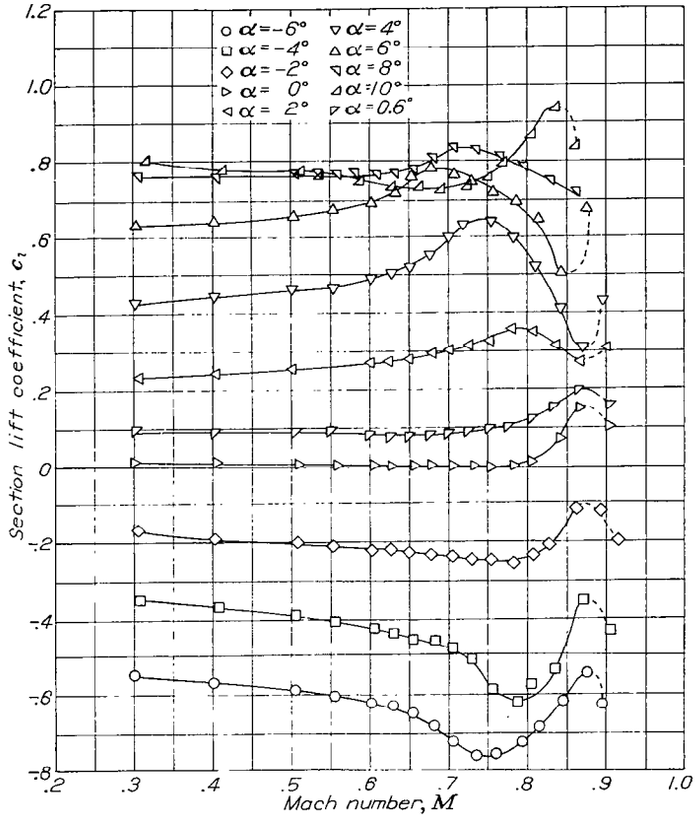

FIGURE 15.—The variation of section lift coefficient with Mach number at various angles of attack for the NACA 836B110 airfoil.

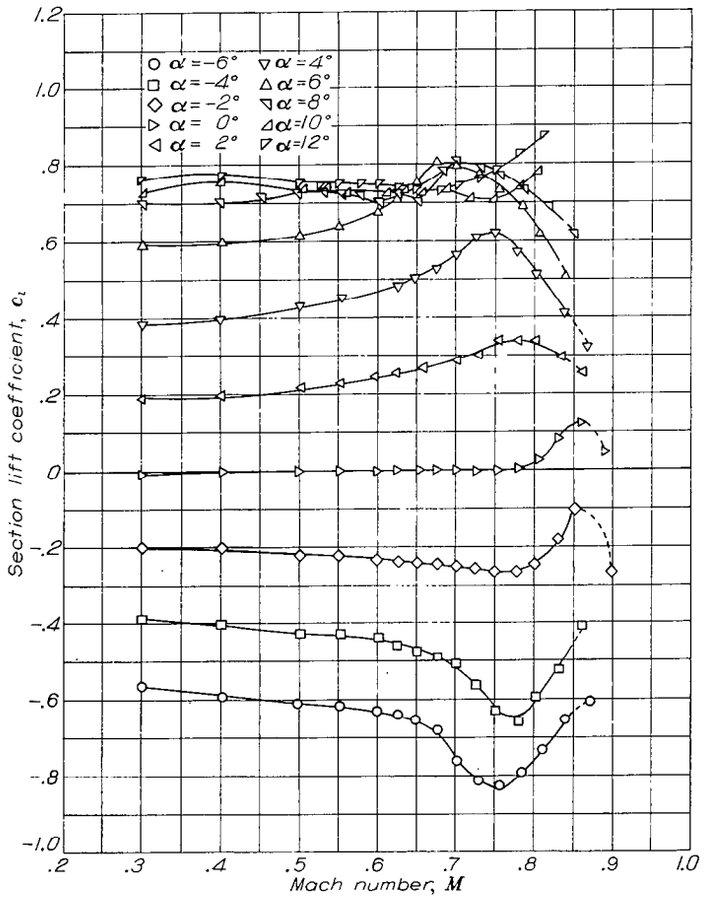

FIGURE 16.—The variation of section lift coefficient with Mach number at various angles of attack for the NACA 836C110 airfoil.

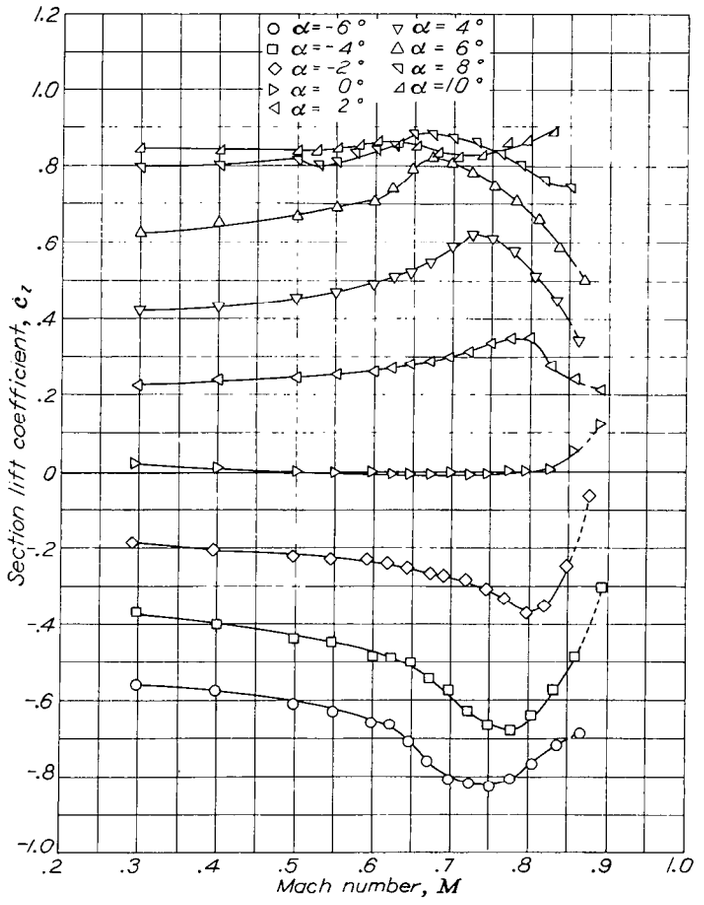

FIGURE 17.—The variation of section lift coefficient with Mach number at various angles of attack for the NACA 836D110 airfoil.

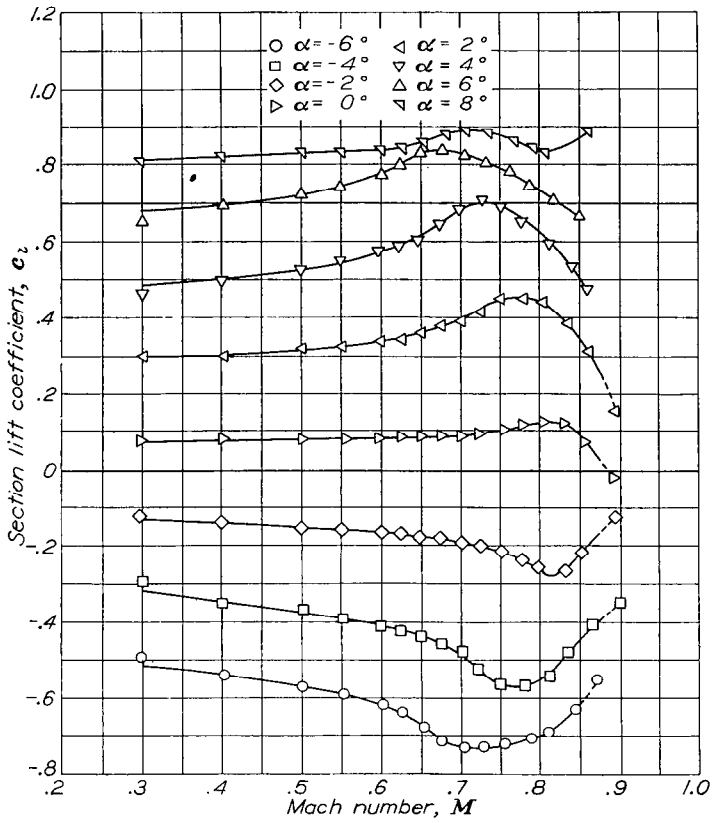

FIGURE 18.—The variation of section lift coefficient with Mach Number at various angles of attack for the NACA 64-110 airfoil.

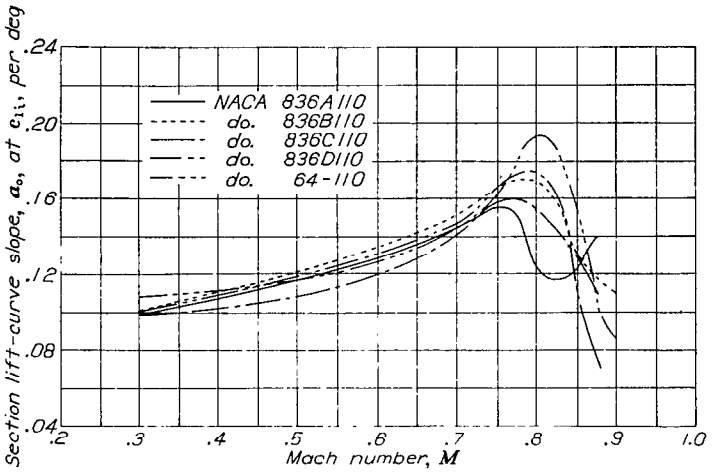

FIGURE 19.—The variation with Mach number of the section lift-curve slope at the design lift coefficient for the NACA 836A110, 836B110, 836C110, 836D110 and the 64-110 airfoils.

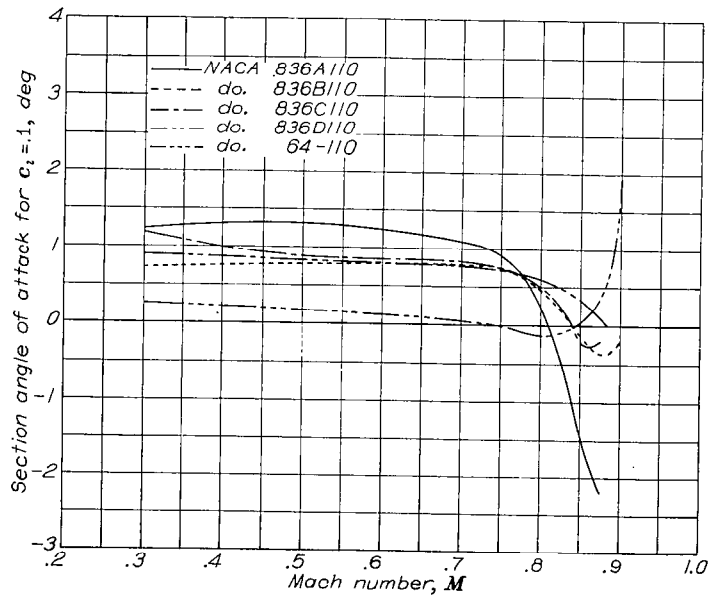

FIGURE 20.—The variation with Mach number of the section angle of attack for a lift coefficient of 0.1 for the NACA 836A110, 836B110, 836C110, 836D110 and 64-110 airfoils.

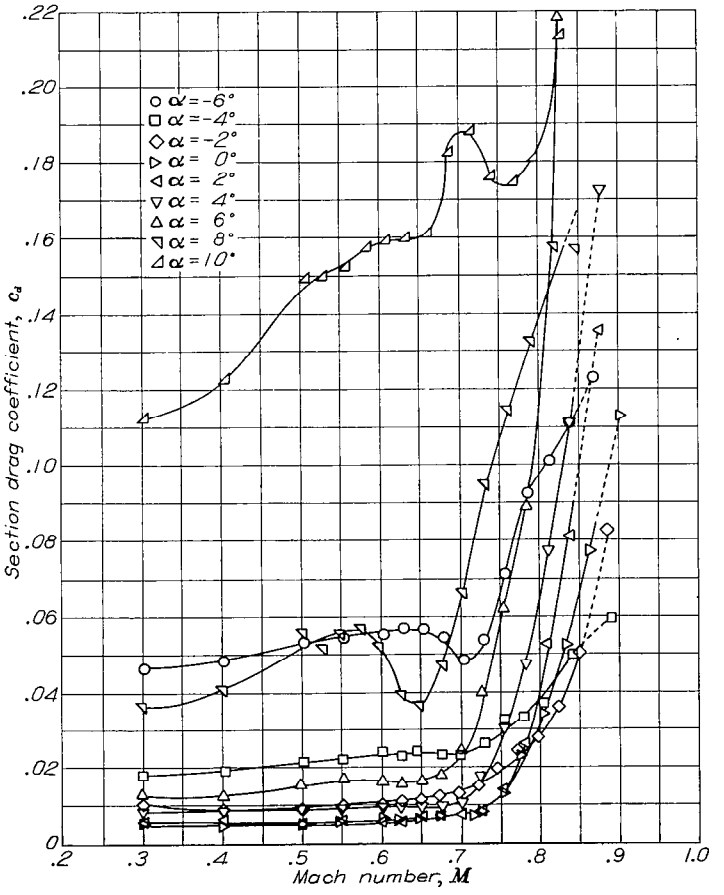

FIGURE 21.—The variation of section drag coefficient with Mach number at various angles of attack for the NACA 836A110 airfoil.

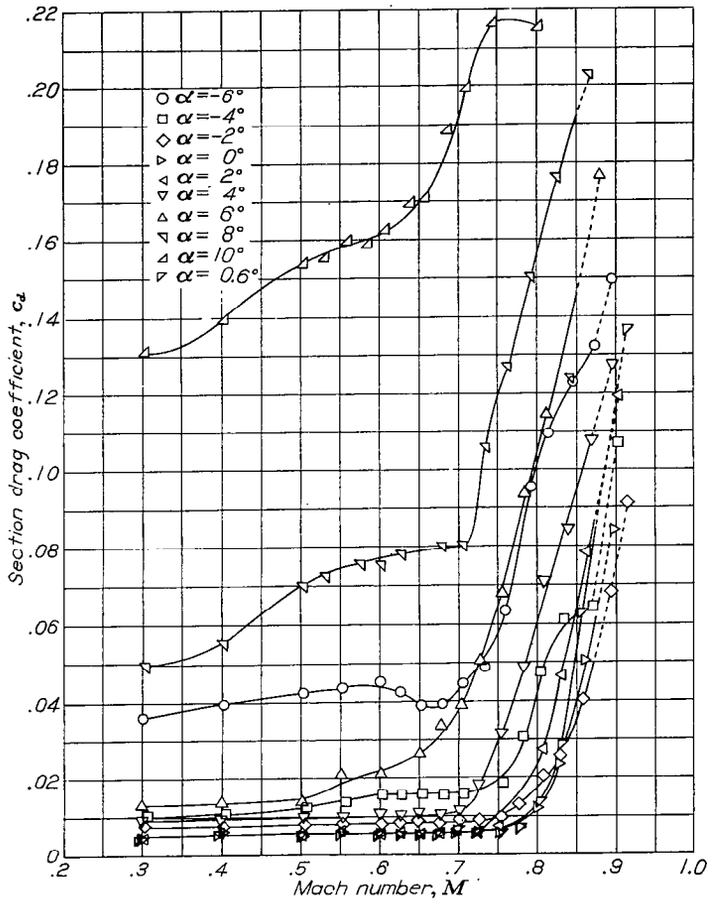

FIGURE 22.—The variation of section drag coefficient with Mach number at various angles of attack for the NACA 836B110 airfoil.

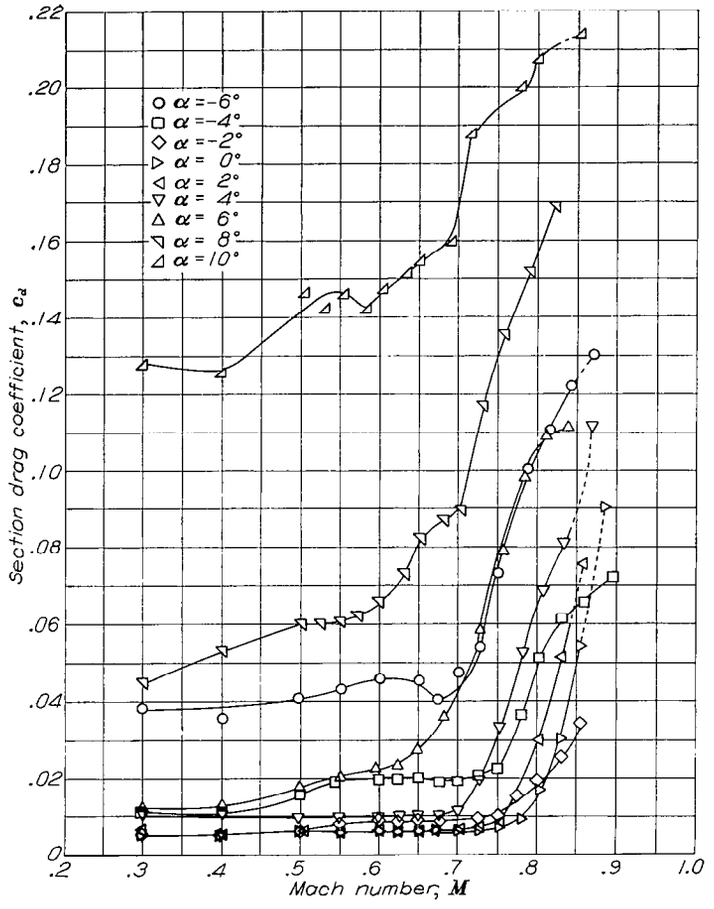

FIGURE 23.—The variation of section drag coefficient with Mach number at various angles of attack for the NACA 836C110 airfoil.

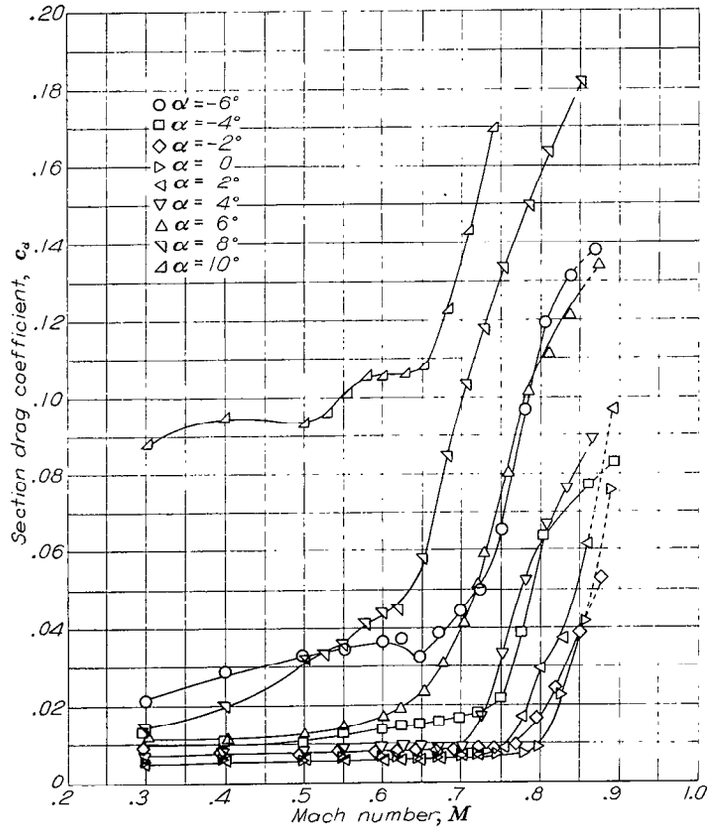

FIGURE 24.—The variation of section drag coefficient with Mach number at various angles of attack for the NACA 836D110 airfoil.

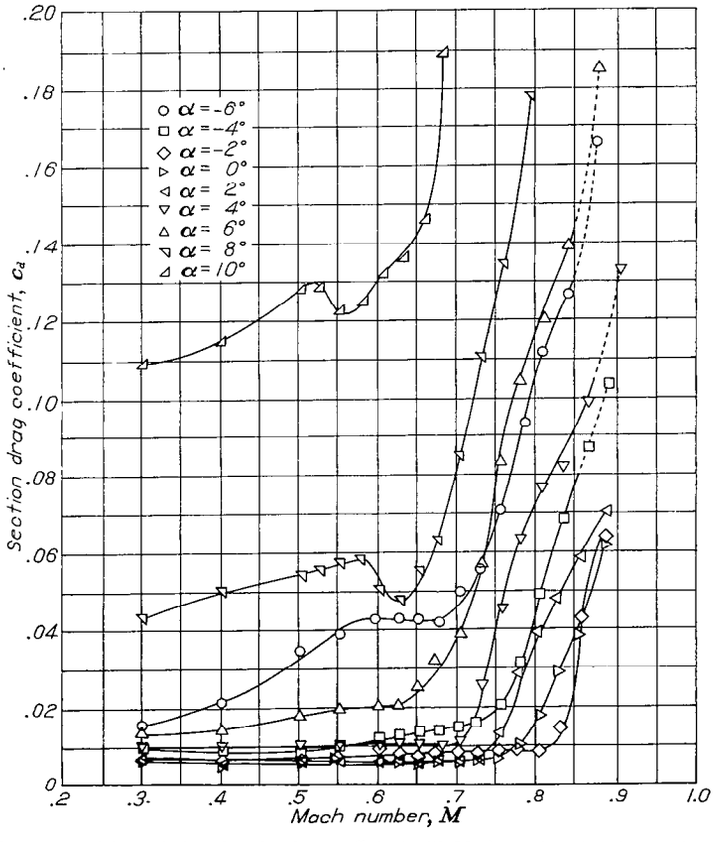

FIGURE 25.—The variation of section drag coefficient with Mach number at various angles of attack for the NACA 65-210 airfoil.

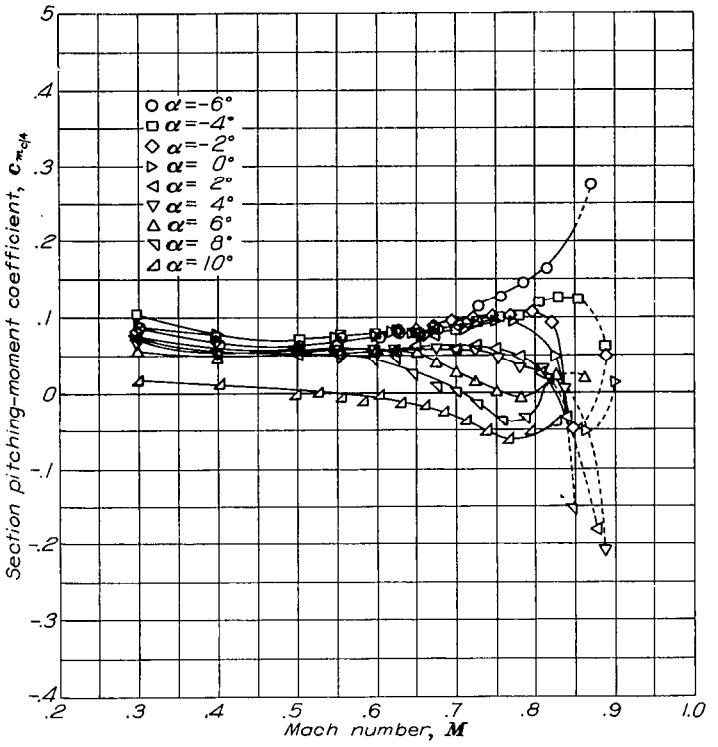

FIGURE 26.—The variation of section quarter-chord moment coefficient with Mach number at various angles of attack for the NACA 836A110 airfoil.

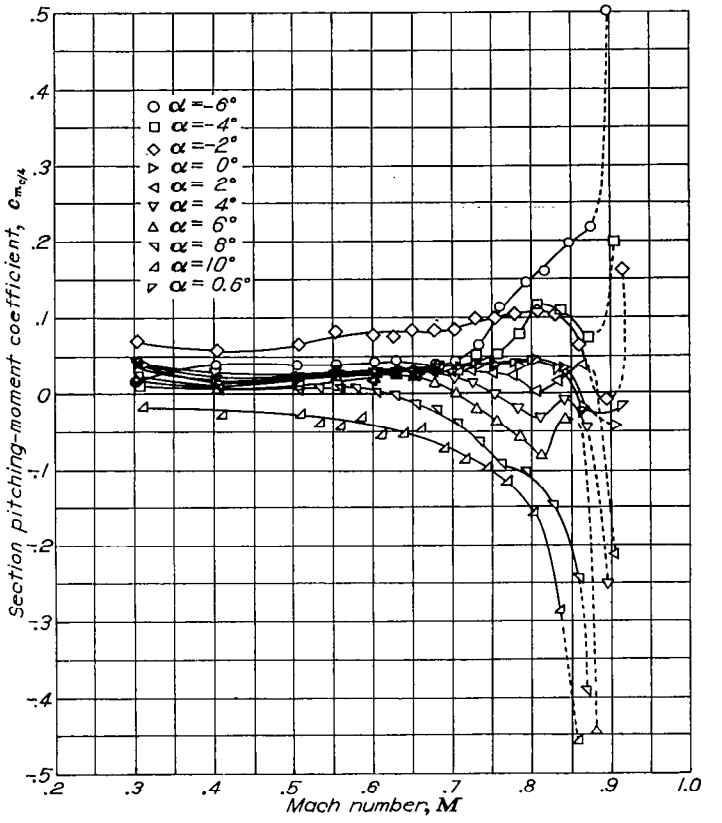

FIGURE 27.—The variation of section quarter-chord moment coefficient with Mach number at various angles of attack for the NACA 836B110 airfoil.

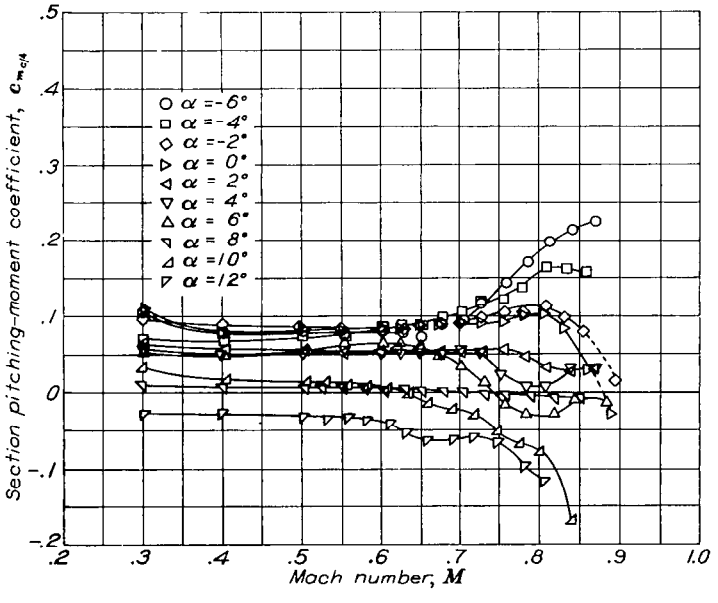

FIGURE 28.—The variation of section quarter-chord moment coefficient with Mach number at various angles of attack for the NACA 836C110 airfoil.

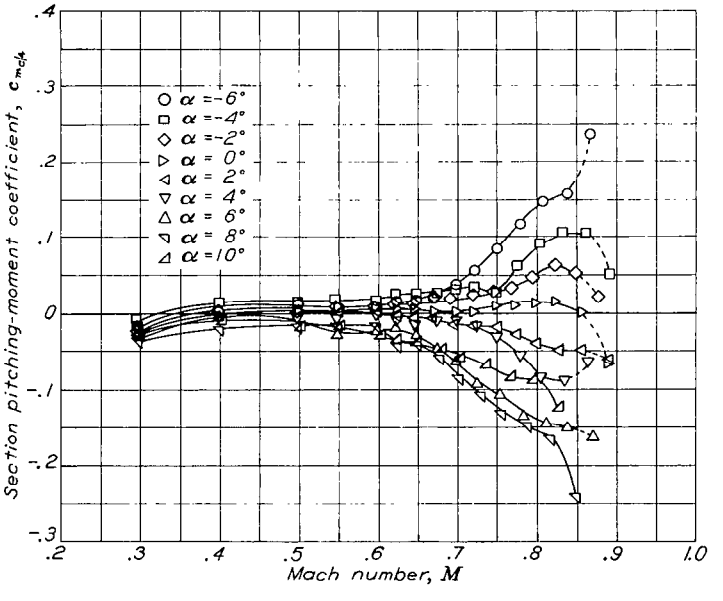

FIGURE 29.—The variation of section quarter-chord moment coefficient with Mach number at various angles of attack for the NACA 836D110 airfoil.

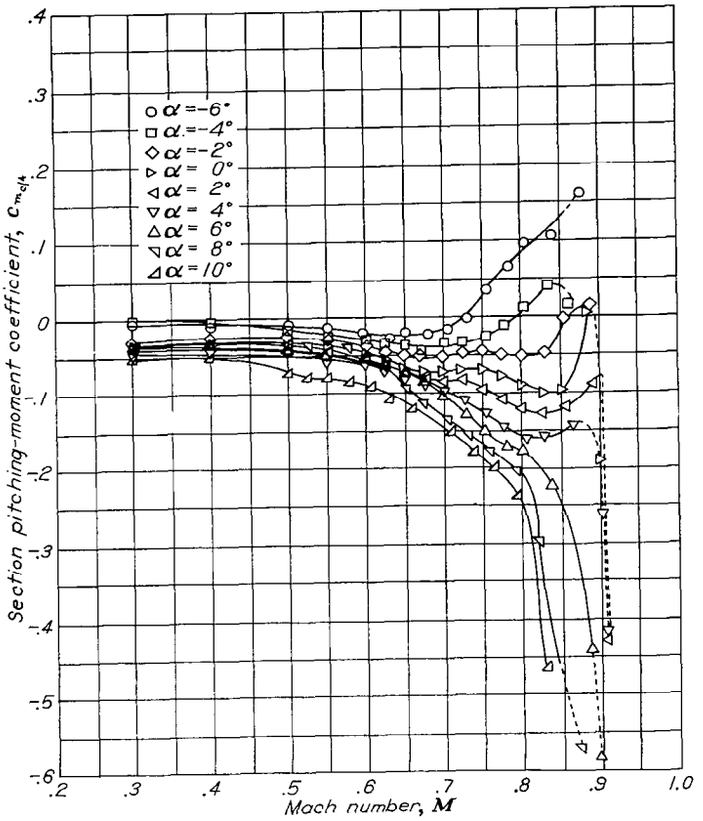

FIGURE 30.—The variation of section quarter-chord moment coefficient with Mach number at various angles of attack for the NACA 65-210 airfoil.

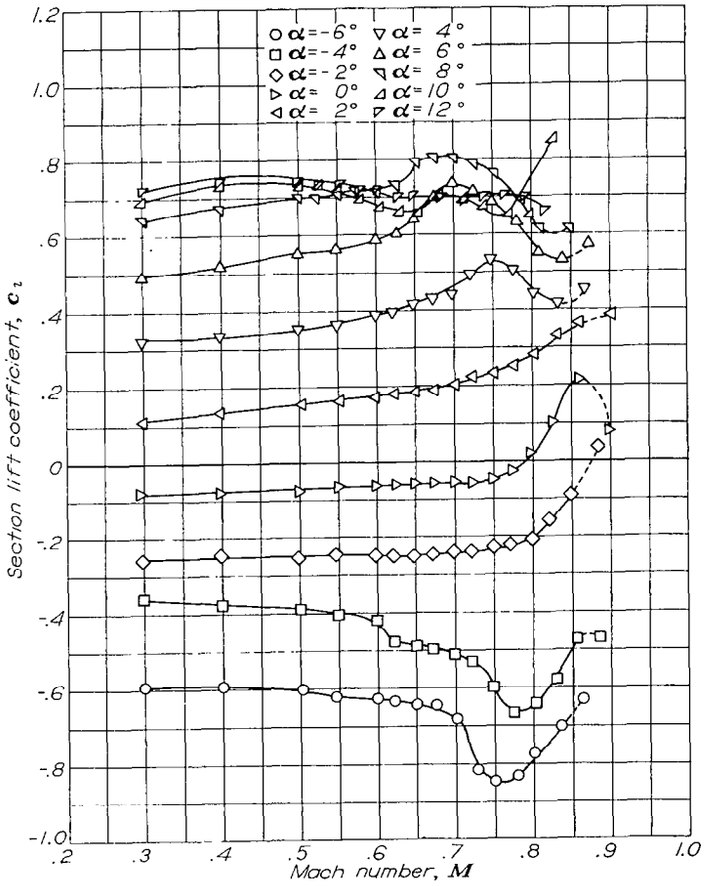

FIGURE 31.—The variation of section lift coefficient with Mach number at various angles of attack for the NACA 847A110 airfoil.

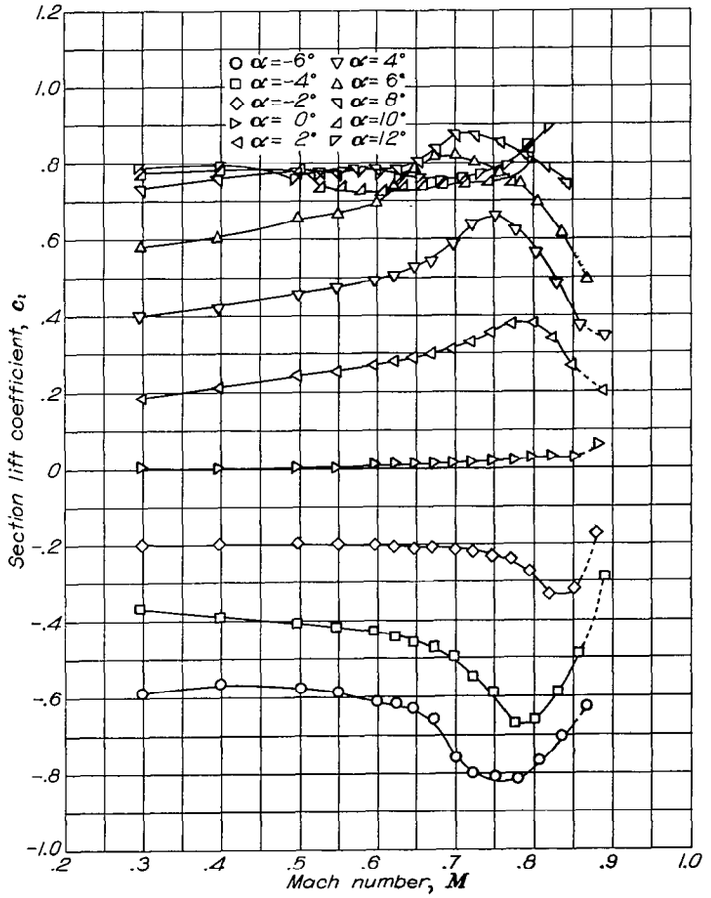

FIGURE 32.—The variation of section lift coefficient with Mach number at various angles of attack for the NACA 847B110 airfoil.

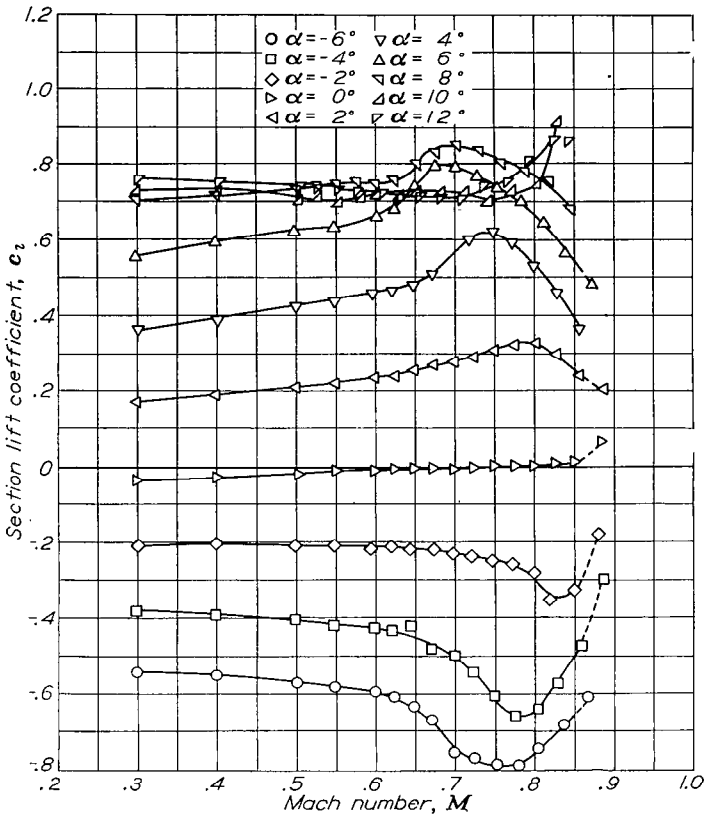

FIGURE 33.—The variation of section lift coefficient with Mach number at various angles of attack for the NACA 847C110 airfoil.

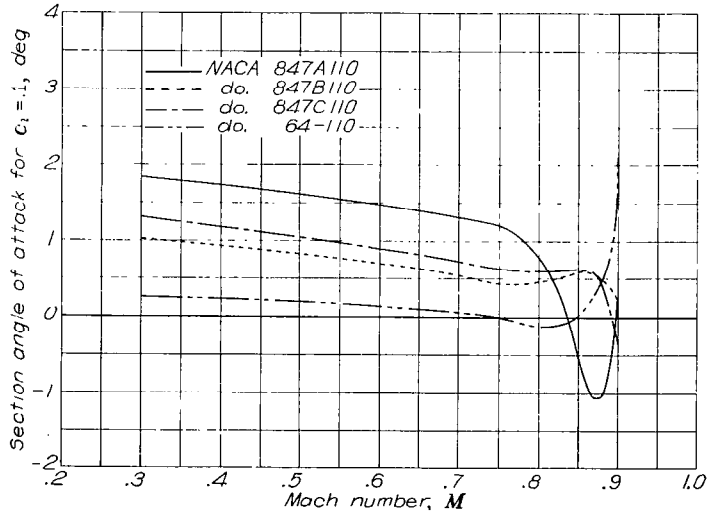

FIGURE 35.—The variation with Mach number of the section angle of attack for a lift coefficient of 0.1 for the NACA 847A110, 847B110, 847C110, and 64-110 airfoils.

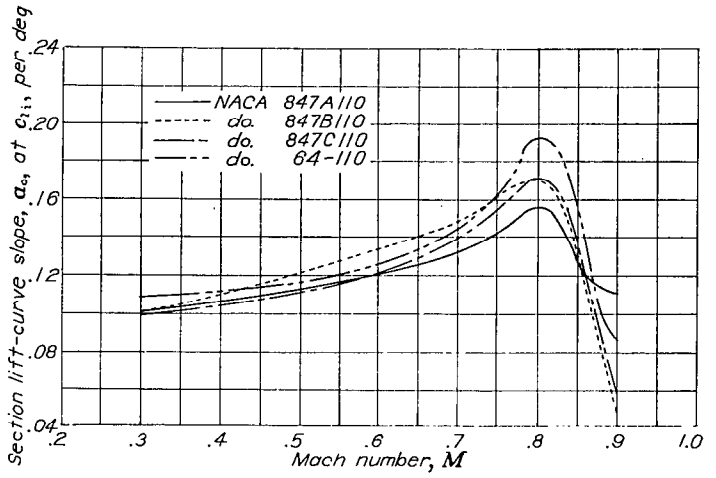

FIGURE 34.—The variation with Mach number of the section lift-curve slope at the design lift coefficient for the NACA 847A110, 847B110, 847C110 and 64-110 airfoils.

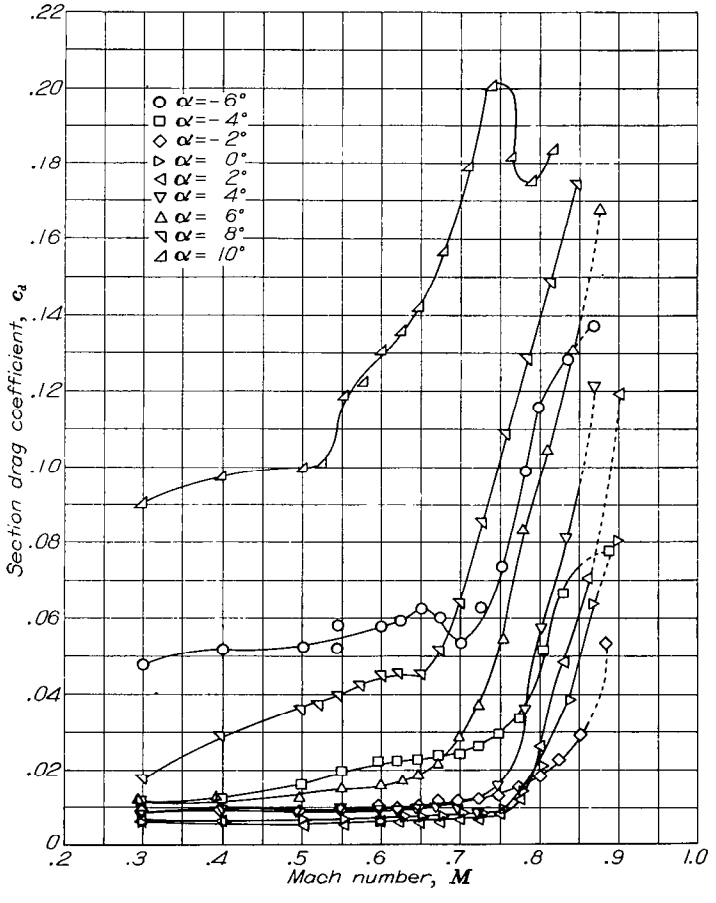

FIGURE 36.—The variation of section drag coefficient with Mach number at various angles of attack for the NACA 847A110 airfoil.

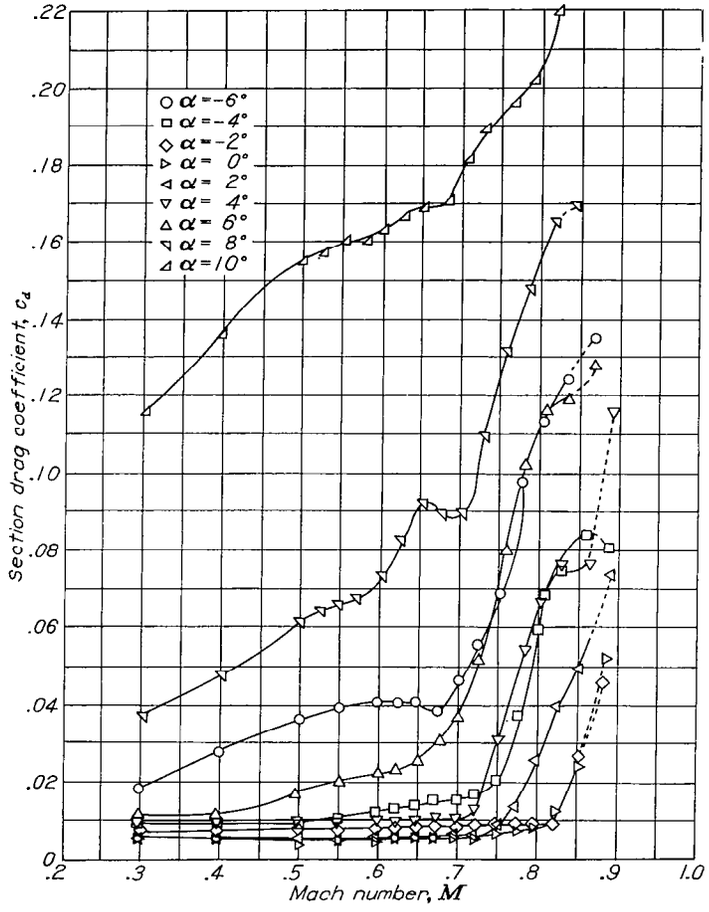

FIGURE 37.—The variation of section drag coefficient with Mach number at various angles of attack for the NACA 847B110 airfoil.

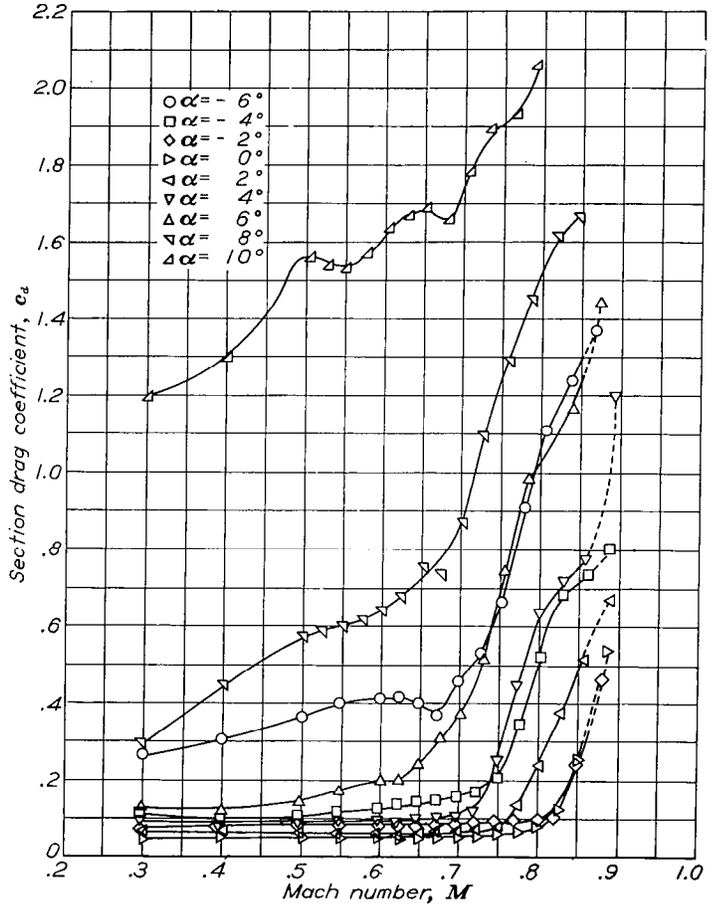

FIGURE 38.—The variation of section drag coefficient with Mach number at various angles of attack for the NACA 847C110 airfoil.

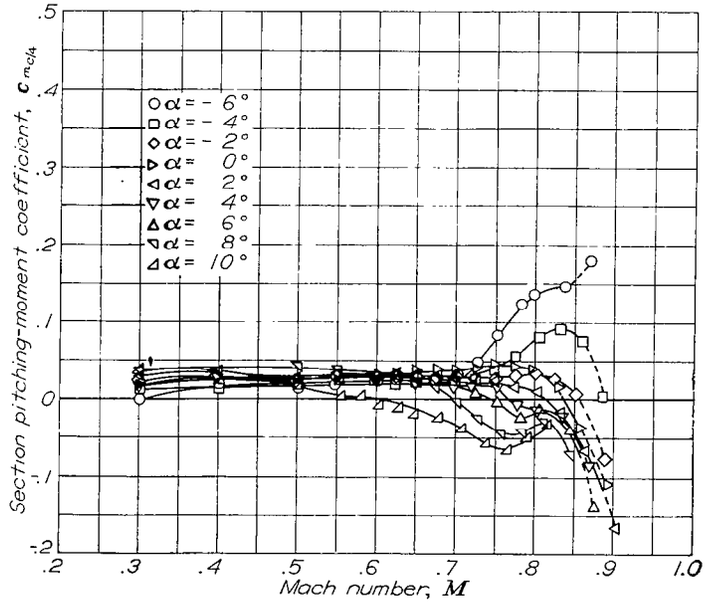

FIGURE 39.—The variation of section quarter-chord moment coefficient with Mach number at various angles of attack for the NACA 847A110 airfoil.

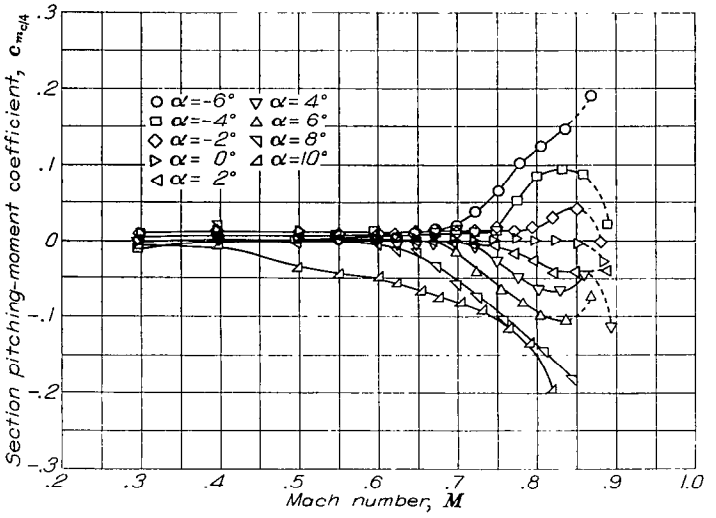

FIGURE 40.—The variation of section quarter-chord moment coefficient with Mach number at various angles of attack for the NACA 847B110 airfoil.

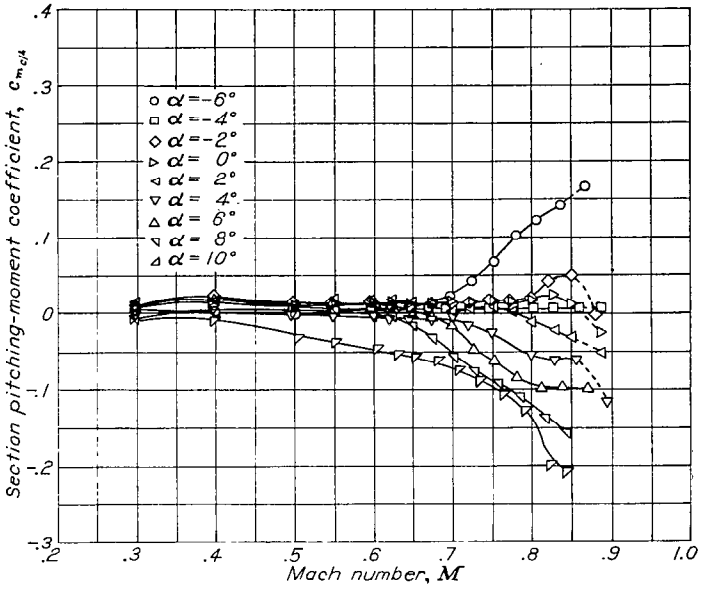

FIGURE 41.—The variation of section quarter-chord moment coefficient with Mach number at various angles of attack for the NACA 847C110 airfoil.

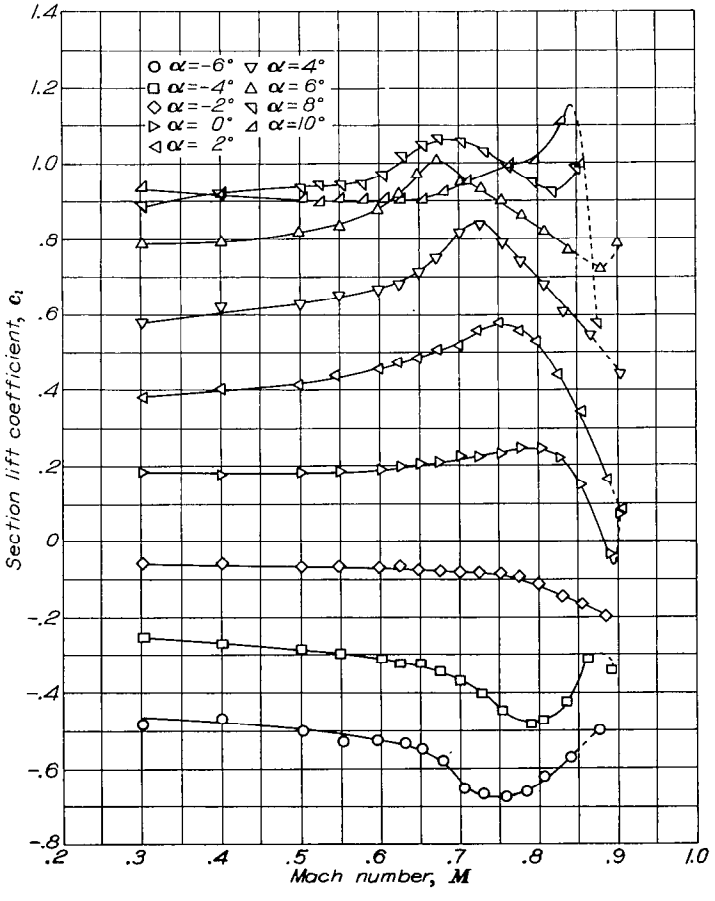

FIGURE 42.—The variation of section lift coefficient with Mach number at various angles of attack for the NACA 65-210 airfoil with a 20-percent-chord plain flap. δ_f,0°.

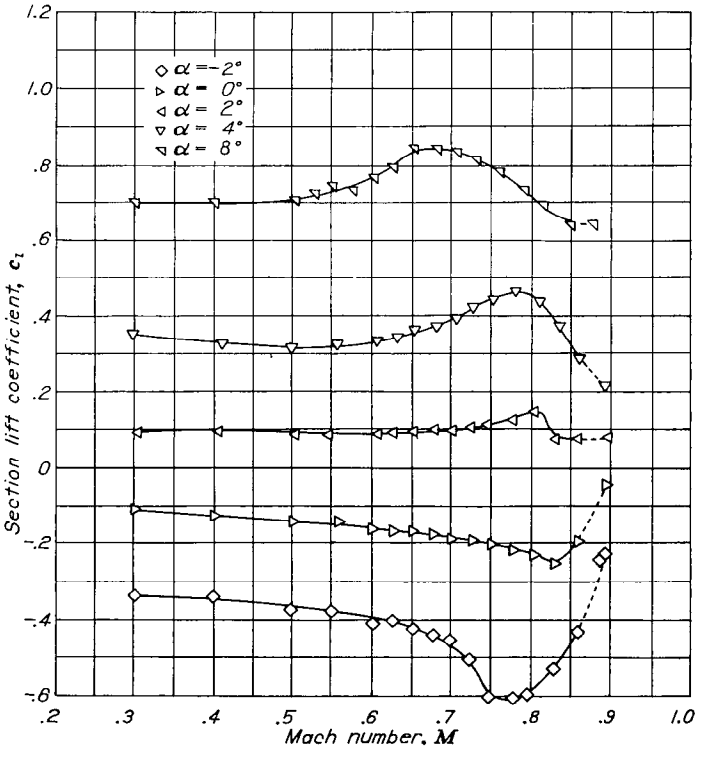

FIGURE 43.—The variation of section lift coefficient with Mach number at various angles of attack for the NACA 65-210 airfoil with a 20-percent-chord plain flap. δ_f,−6°.

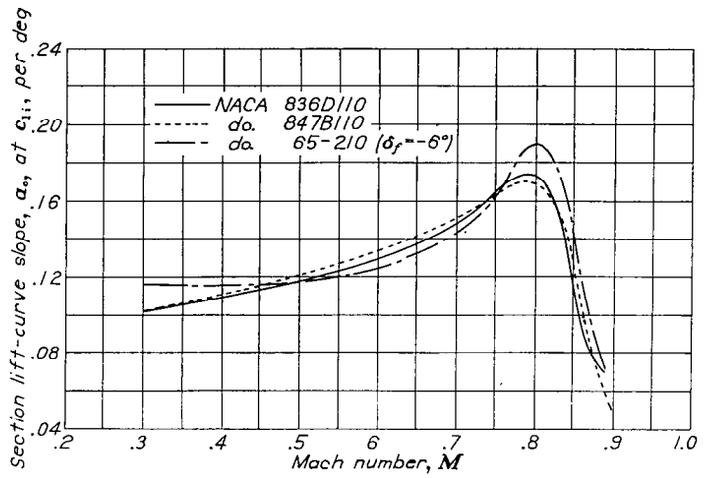

FIGURE 44.—The variation with Mach number of the section lift-curve slope at a lift coefficient of 0.1 for the NACA 65-210 ($\delta_f = -6°$), 836D110 and 847B110 airfoils.

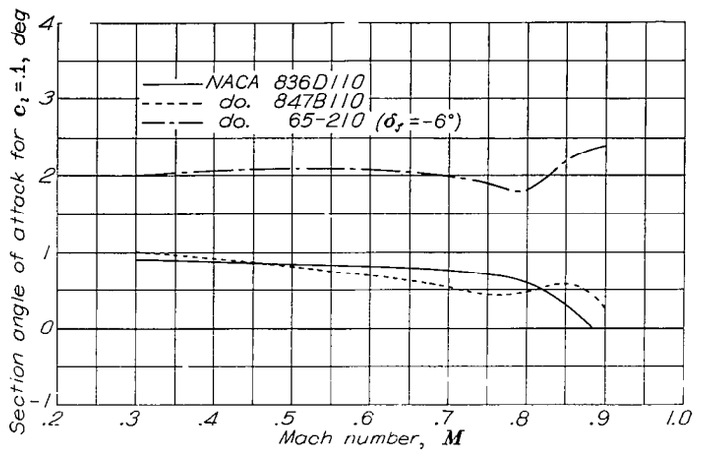

FIGURE 45.—The variation with Mach number of the angle of attack for a lift coefficient of 0.1 for the NACA 65-210 ($\delta_f = -6°$), 836D110 and 847B110 airfoils.

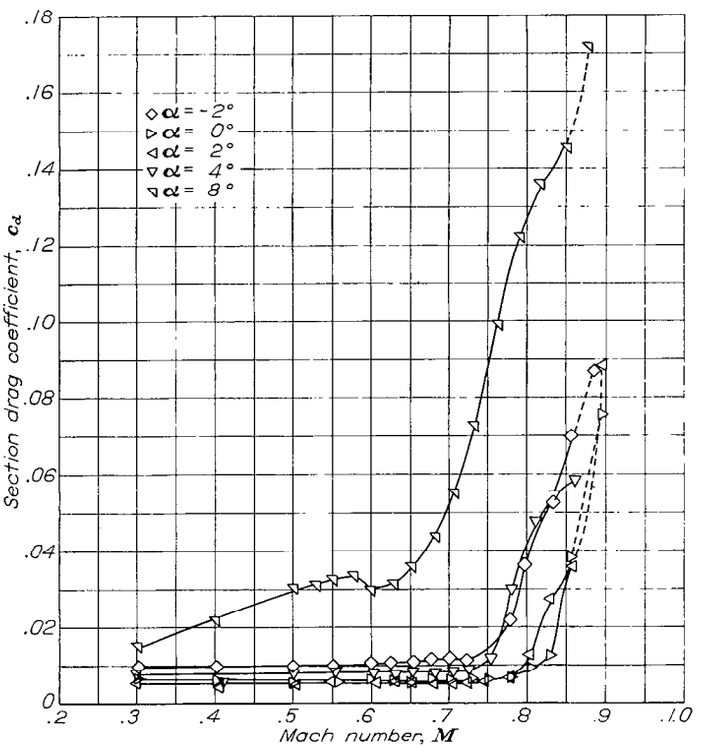

FIGURE 46.—The variation of section drag coefficient with Mach number at various angles of attack for the NACA 65-210 airfoil with a 20-percent-chord plain flap. δ_f,−6°.

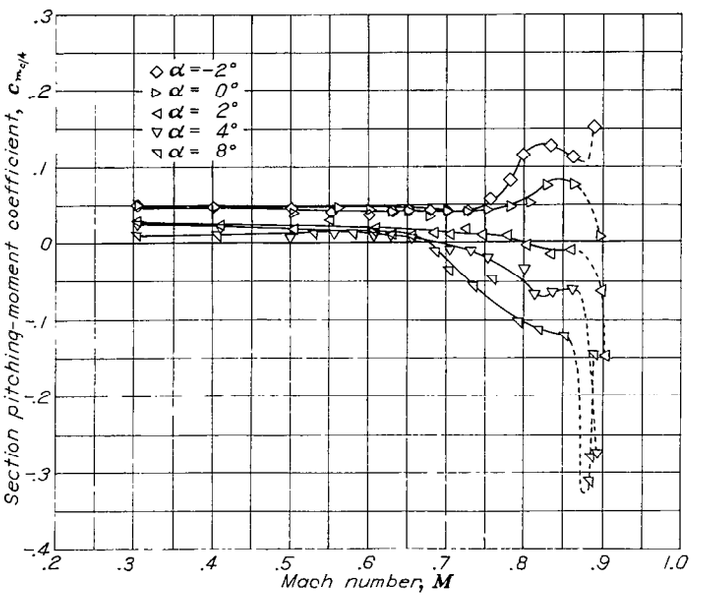

FIGURE 47.—The variation of section quarter-chord moment coefficient at various angles of attack for the NACA 65-210 airfoil with a 20-percent-chord plain flap. δ_f,−6°.

TABLE I.—COORDINATES FOR THE NACA 835A216 AIRFOIL

[Stations and ordinates given in percent of airfoil chord

Upper surface		Lower surface	
Station	Ordinate	Station	Ordinate
0	0	0	0
.321	1.090	.679	−.890
.550	1.342	.950	−1.054
1.030	1.734	1.470	−1.292
2.268	2.474	2.732	−1.714
4.793	3.591	5.207	−2.391
7.342	4.453	7.658	−2.979
9.901	5.162	10.099	−3.528
15.034	6.264	14.966	−4.554
20.186	7.036	19.814	−5.506
25.369	7.523	24.631	−6.405
30.589	7.714	29.411	−7.246
35.832	7.567	34.168	−8.023
40.881	7.154	39.119	−8.748
45.574	6.687	44.426	−9.203
50.234	6.189	49.766	−9.239
54.967	5.666	55.033	−8.812
59.778	5.123	60.222	−8.037
64.675	4.567	65.325	−7.027
69.664	4.010	70.336	−5.831
74.713	3.436	75.287	−4.552
79.793	2.834	80.207	−3.246
84.883	2.205	85.117	−1.989
89.963	1.540	90.037	−.878
95.009	.821	94.991	−.072
100.000	0	100.000	0

L. E. radius: 1.121
Slope through L. E.: 0.191

TABLE II.—COORDINATES FOR THE NACA 836A216 AIRFOIL

[Stations and ordinates given in percent of airfoil chord]

Upper surface		Lower surface	
Station	Ordinate	Station	Ordinate
0	0	0	0
.303	1.145	.697	−.927
.530	1.402	.970	−1.092
1.006	1.790	1.494	−1.314
2.232	2.541	2.768	−1.715
4.735	3.680	5.265	−2.326
7.266	4.580	7.734	−2.852
9.816	5.344	10.184	−3.354
14.945	6.522	15.055	−4.276
20.094	7.359	19.906	−5.139
25.279	7.904	24.721	−5.960
30.533	8.134	29.467	−6.742
35.780	8.004	34.220	−7.484
40.900	7.620	39.100	−8.186
45.910	7.085	44.090	−8.803
50.822	6.453	49.178	−9.273
55.625	5.769	54.375	−9.533
60.311	5.067	59.689	−9.469
64.912	4.374	65.088	−8.934
69.627	3.703	70.373	−7.855
74.560	3.100	75.440	−6.450
79.605	2.515	80.395	−4.873
84.735	1.945	85.265	−3.239
89.873	1.342	90.127	−1.688
94.981	.707	95.019	−.433
100.000	0	100.000	0

L. E. radius: 1.183
Slope through L. E.: 0.208

TABLE III.—COORDINATES FOR THE NACA 847A216 AIRFOIL

[Stations and ordinates given in percent of airfoil chord]

Upper surface		Lower surface	
Station	Ordinate	Station	Ordinate
0	0	0	0
.280	1.169	.720	−.949
.501	1.430	.999	−1.108
.962	1.873	1.538	−1.359
2.176	2.677	2.824	−1.763
4.673	3.830	5.327	−2.294
7.192	4.738	7.808	−2.732
9.720	5.490	10.280	−3.118
14.801	6.692	15.199	−3.816
19.905	7.606	20.095	−4.464
25.027	8.279	24.973	−5.079
30.170	8.734	29.830	−5.670
35.352	8.968	34.648	−6.244
40.605	8.920	39.395	−6.810
45.825	8.556	44.175	−7.358
50.931	7.962	49.069	−7.880
55.909	7.226	54.091	−8.328
60.786	6.405	59.214	−8.626
65.561	5.545	64.439	−8.697
70.189	4.697	69.811	−8.409
74.731	3.873	75.239	−7.525
79.569	3.110	80.431	−6.050
84.635	2.367	85.365	−4.261
89.790	1.602	90.210	−2.404
94.952	.820	95.048	−.740
100.000	0	100.000	0

L. E. radius: 1.242
Slope through L. E.: 0.220

TABLE IV.—COORDINATES FOR THE NACA 836A110 AIRFOIL

[Stations and ordinates given in percent of airfoil chord]

Upper surface		Lower surface	
Station	Ordinate	Station	Ordinate
0	0	0	0
.426	.700	.575	−.539
.662	.861	.831	−.672
1.145	1.110	1.336	−.815
2.378	1.578	2.585	−1.078
4.881	2.262	5.076	−1.480
7.392	2.818	7.573	−1.810
9.909	3.297	10.045	−2.117
14.958	4.033	14.997	−2.680
20.017	4.594	19.940	−3.217
25.089	4.917	24.839	−3.732
30.189	5.072	29.772	−4.226
35.286	5.009	34.677	−4.703
40.334	4.788	39.632	−5.162
45.342	4.475	44.627	−5.554
50.309	4.108	49.663	−5.870
55.255	3.699	54.721	−6.047
60.113	3.279	59.887	−6.025
64.956	2.836	65.023	−5.707
69.843	2.465	70.144	−5.052
74.816	2.093	75.174	−4.177
79.835	1.722	80.157	−3.187
84.888	1.345	85.107	−2.145
89.946	.935	90.052	−1.144
94.992	.493	95.007	−.318
100.000	0	100.000	0

L. E. radius: 0.498
Slope through L. E.: 0.119

TABLE V.—COORDINATES FOR THE NACA 836B110 AIRFOIL

[Stations and ordinates given in percent of airfoil chord]

Upper surface		Lower surface	
Station	Ordinate	Station	Ordinate
0	0	0	0
.371	.734	.481	−.643
.600	.893	.724	−.765
1.075	1.143	1.215	−.943
2.302	1.580	2.454	−1.238
4.808	2.228	4.954	−1.679
7.321	2.750	7.463	−2.035
9.850	3.195	9.968	−2.347
14.925	3.902	14.991	−2.889
20.015	4.428	20.019	−3.356
25.125	4.808	25.053	−3.768
30.277	5.053	30.101	−4.144
35.425	5.153	35.147	−4.495
40.501	5.128	40.167	−4.779
45.516	5.001	45.168	−4.993
50.469	4.794	50.149	−5.123
55.391	4.519	55.119	−5.145
60.181	4.180	60.045	−5.017
64.963	3.784	64.949	−4.690
69.781	3.326	69.905	−4.134
74.740	2.828	74.892	−3.423
79.768	2.282	79.902	−2.617
84.845	1.707	84.931	−1.771
89.929	1.110	89.963	−.956
94.991	.525	94.993	−.280
100.000	0	100.000	0

L. E. radius: 0.659
Slope through L. E.: 0.095

TABLE VI.—COORDINATES FOR THE NACA 836C110 AIRFOIL

[Stations and ordinates given in percent of airfoil chord]

Upper surface		Lower surface	
Station	Ordinate	Station	Ordinate
0	0	0	0
.371	.734	.481	−.643
.600	.893	.724	−.765
1.075	1.143	1.215	−.943
2.302	1.580	2.454	−1.238
4.808	2.228	4.954	−1.679
7.321	2.750	7.463	−2.035
9.850	3.195	9.968	−2.347
14.925	3.902	14.991	−2.889
20.015	4.428	20.019	−3.356
25.125	4.808	25.053	−3.768
30.277	5.053	30.101	−4.144
35.425	5.153	35.147	−4.485
40.501	5.128	40.167	−4.779
45.516	5.001	45.168	−4.993
50.469	4.794	50.149	−5.123
55.391	4.519	55.119	−5.145
60.181	4.180	60.045	−5.017
64.963	3.784	64.949	−4.690
69.781	3.326	69.905	−4.134
74.740	2.828	74.892	−3.423
79.767	2.335	79.903	−2.670
84.842	1.844	84.934	−1.907
89.925	1.325	89.967	−1.171
94.991	.745	94.994	−.499
100.000	0	100.000	0

L. E. radius: 0.659
Slope through L. E.: 0.095

TABLE VII.—COORDINATES FOR THE NACA 836D110 AIRFOIL

[Station and ordinates given in percent of airfoil chord]

Upper surface		Lower surface	
Station	Ordinate	Station	Ordinate
0	0	0	0
.443	.769	.558	−.678
.681	.937	.812	−.808
1.166	1.204	1.315	−1.004
2.400	1.694	2.564	−1.352
4.898	2.406	5.070	−1.858
7.406	2.959	7.560	−2.244
9.913	3.422	10.041	−2.574
14.942	4.135	15.014	−3.122
19.977	4.650	19.981	−3.578
25.016	5.004	24.942	−3.964
30.071	5.204	29.891	−4.295
35.124	5.238	34.840	−4.570
40.149	5.119	39.817	−4.770
45.155	4.884	44.815	−4.876
50.139	4.558	49.833	−4.887
55.114	4.160	54.862	−4.786
60.051	3.709	59.929	−4.547
64.995	3.251	64.997	−4.157
69.941	2.793	70.047	−3.601
74.932	2.325	75.058	−2.920
79.941	1.847	80.051	−2.182
84.964	1.366	85.032	−1.430
89.985	.885	90.013	−.732
95.001	.427	94.999	−.182
100.000	0	100.000	0

L. E. radius: 0.618
Slope through L. E.: 0.098

TABLE VIII.—COORDINATES FOR THE NACA 847A110 AIRFOIL

[Station and ordinates given in percent of airfoil chord]

Upper surface		Lower surface	
Station	Ordinate	Station	Ordinate
0	0	0	0
.429	.738	.571	−.628
.669	.902	.831	−.740
1.157	1.173	1.343	−.915
2.396	1.652	2.604	−1.194
4.896	2.324	5.104	−1.556
7.403	2.857	7.597	−1.853
9.912	3.298	10.088	−2.112
14.938	4.010	15.062	−2.572
19.970	4.563	20.030	−2.991
25.008	4.975	24.992	−3.375
30.053	5.267	29.947	−3.735
35.110	5.437	34.890	−4.075
40.190	5.454	39.810	−4.398
45.259	5.297	44.741	−4.697
50.293	5.001	49.707	−4.959
55.286	4.620	54.714	−5.172
60.248	4.188	59.752	−5.298
65.178	3.729	64.822	−5.305
70.060	3.246	69.940	−5.102
74.923	2.753	75.077	−4.579
79.859	2.236	80.141	−3.706
84.880	1.697	85.120	−2.645
89.930	1.134	90.070	−1.536
94.984	.548	95.016	−.508
100.000	0	100.000	0

L. E. radius: 0.590
Slope through L. E.: 0.104

TABLE IX.—COORDINATES FOR THE NACA 847B110 AIRFOIL

[Stations and ordinates given in percent of airfoil chord]

Upper surface		Lower surface	
Station	Ordinate	Station	Ordinate
0	0	0	0
.445	.792	.555	−.711
.688	.964	.812	−.847
1.179	1.239	1.321	−1.055
2.420	1.723	2.580	−1.400
4.918	2.413	5.082	−1.871
7.421	2.947	7.579	−2.233
9.926	3.390	10.074	−2.537
14.942	4.095	15.058	−3.038
19.962	4.631	20.038	−3.447
24.985	5.031	25.015	−3.784
30.011	5.309	29.989	−4.057
35.044	5.467	34.956	−4.270
40.087	5.490	39.913	−4.426
45.124	5.346	44.876	−4.498
50.141	5.072	49.859	−4.499
55.137	4.705	54.863	−4.433
60.119	4.273	59.881	−4.293
65.087	3.796	64.913	−4.069
70.037	3.280	69.963	−3.722
74.982	2.741	75.018	−3.207
79.957	2.179	80.043	−2.517
84.965	1.606	85.035	−1.744
89.982	1.033	90.018	−.976
94.999	.477	95.001	−.299
100.000	0	100.000	0

L. E. radius: 0.693
Slope through L. E.: 0.080

TABLE X.—COORDINATES FOR THE NACA 847C110 AIRFOIL

[Stations and ordinates given in percent of airfoil chord]

Upper surface		Lower surface	
Station	Ordinate	Station	Ordinate
0	0	0	0
.445	.792	.555	−.711
.688	.964	.812	−.847
1.179	1.239	1.321	−1.055
2.420	1.723	2.580	−1.400
4.918	2.413	5.082	−1.871
7.421	2.947	7.579	−2.233
9.926	3.390	10.074	−2.537
14.942	4.095	15.058	−3.038
19.962	4.631	20.038	−3.447
24.985	5.031	25.015	−3.784
30.011	5.309	29.989	−4.057
35.044	5.467	34.956	−4.270
40.087	5.490	39.913	−4.426
45.124	5.346	44.876	−4.498
50.141	5.072	49.859	−4.499
55.137	4.705	54.863	−4.433
60.119	4.273	59.881	−4.293
65.087	3.796	64.913	−4.069
70.037	3.280	69.963	−3.722
74.982	2.741	75.018	−3.207
79.957	2.210	80.043	−2.548
84.963	1.716	85.037	−1.853
89.979	1.218	90.021	−1.161
94.998	.684	95.002	−.506
100.000	0	100.000	0

L. E. radius: 0.693
Slope through L. E.: 0.080

U. S. GOVERNMENT PRINTING OFFICE: 1950

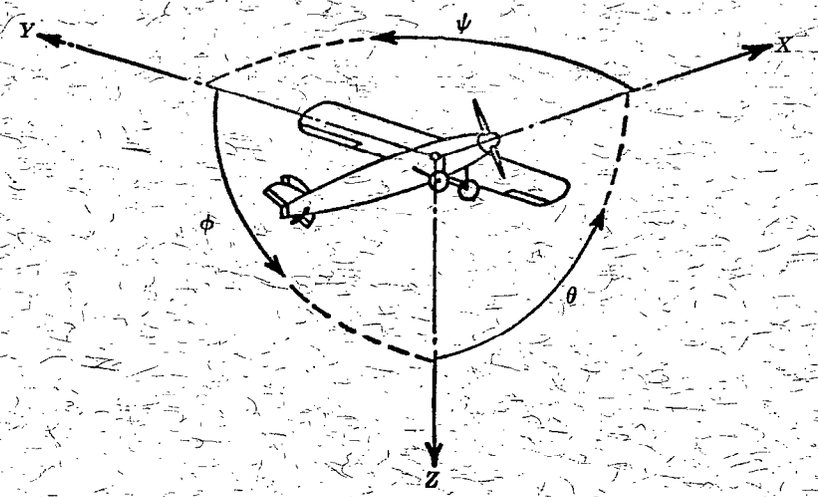

Positive directions of axes and angles (forces and moments) are shown by arrows

Axis		Force (parallel to axis) symbol	Moment about axis			Angle		Velocities	
Designation	Symbol		Designation	Symbol	Positive direction	Designation	Symbol	Linear (component along axis)	Angular
Longitudinal	X	X	Rolling	L	$Y \longrightarrow Z$	Roll	ϕ	u	p
Lateral	Y	Y	Pitching	M	$Z \longrightarrow X$	Pitch	θ	v	q
Normal	Z	Z	Yawing	N	$X \longrightarrow Y$	Yaw	ψ	w	r

Absolute coefficients of moment

$C_l = \frac{L}{qbS}$ (rolling) $\quad C_m = \frac{M}{qcS}$ (pitching) $\quad C_n = \frac{N}{qbS}$ (yawing)

Angle of set of control surface (relative to neutral position), δ. (Indicate surface by proper subscript.)

4. PROPELLER SYMBOLS

D Diameter

p Geometric pitch

p/D Pitch ratio

V' Inflow velocity

V_s Slipstream velocity

T Thrust, absolute coefficient $C_T = \frac{T}{\rho n^2 D^4}$

Q Torque, absolute coefficient $C_Q = \frac{Q}{\rho n^2 D^5}$

P Power, absolute coefficient $C_P = \frac{P}{\rho n^3 D^5}$

C_s Speed-power coefficient $= \sqrt[5]{\frac{\rho V^5}{P n^2}}$

η Efficiency

n Revolutions per second, rps

Φ Effective helix angle $= \tan^{-1}\left(\frac{V}{2\pi r n}\right)$

5. NUMERICAL RELATIONS

1 hp = 76.04 kg-m/s = 550 ft-lb/sec

1 metric horsepower = 0.9863 hp

1 mph = 0.4470 mps

1 mps = 2.2369 mph

1 lb = 0.4536 kg

1 kg = 2.2046 lb

1 mi = 1,609.35 m = 5,280 ft

1 m = 3.2808 ft